Molecular Therapy
Nucleic Acids
Original Article

Nuclear-Encoded lncRNA *MALAT1* Epigenetically Controls Metabolic Reprogramming in HCC Cells through the Mitophagy Pathway

Yijing Zhao,[1,2] Lei Zhou,[1] Hui Li,[1] Tingge Sun,[1] Xue Wen,[1] Xueli Li,[1] Ying Meng,[1,2] Yan Li,[1,2] Mengmeng Liu,[1,2] Shanshan Liu,[1,2] Su-Jeong Kim,[3] Jialin Xiao,[3] Lingyu Li,[1] Songling Zhang,[1] Wei Li,[1] Pinchas Cohen,[3] Andrew R. Hoffman,[2] Ji-Fan Hu,[1,2] and Jiuwei Cui[1]

[1]Key Laboratory of Organ Regeneration and Transplantation of Ministry of Education, Cancer Center, The First Hospital of Jilin University, Changchun, Jilin 130021, China; [2]Department of Medicine, PAVIR, Stanford University Medical School, VA Palo Alto Health Care System, Palo Alto, CA 94304, USA; [3]Leonard Davis School of Gerontology, University of Southern California, Los Angeles, CA 90089, USA

Mitochondrial dysfunction is a metabolic hallmark of cancer cells. In search of molecular factors involved in this dysregulation in hepatocellular carcinoma (HCC), we found that the nuclear-encoded long noncoding RNA (lncRNA) *MALAT1* (metastasis-associated lung adenocarcinoma transcript 1) was aberrantly enriched in the mitochondria of hepatoma cells. Using RNA reverse transcription-associated trap sequencing (RAT-seq), we showed that *MALAT1* interacted with multiple loci on mitochondrial DNA (mtDNA), including D-loop, *COX2*, *ND3*, and *CYTB* genes. *MALAT1* knockdown induced alterations in the CpG methylation of mtDNA and in mitochondrial transcriptomes. This was associated with multiple abnormalities in mitochondrial function, including altered mitochondrial structure, low oxidative phosphorylation (OXPHOS), decreased ATP production, reduced mitophagy, decreased mtDNA copy number, and activation of mitochondrial apoptosis. These alterations in mitochondrial metabolism were associated with changes in tumor phenotype and in pathways involved in cell mitophagy, mitochondrial apoptosis, and epigenetic regulation. We further showed that the RNA-shuttling protein HuR and the mitochondria transmembrane protein MTCH2 mediated the transport of *MALAT1* in this nuclear-mitochondrial crosstalk. This study provides the first evidence that the nuclear genome-encoded lncRNA *MALAT1* functions as a critical epigenetic player in the regulation of mitochondrial metabolism of hepatoma cells, laying the foundation for further clarifying the roles of lncRNAs in tumor metabolic reprogramming.

INTRODUCTION

Dysregulation of cellular energetics has long been recognized as one of the hallmarks of malignancy, including hepatocellular carcinoma (HCC),[1,2] as changes in mitochondrial bioenergetics, biosynthesis, and signaling are essential requirements for tumorigenesis.[3] Cancer cells ferment glucose as the major metabolic pathway for proliferation even in the presence of oxygen, a paradoxical process known as aerobic glycolysis or the Warburg effect.[4,5] The high level of reactive oxygen species (ROS) found in cancer cells induces genomic instability and ultimately tumorigenesis.[6,7] Targeting this abnormal energy metabolism in cancer cells may become an important strategy in developing novel cancer therapeutics.

Long noncoding RNAs (lncRNAs) are critical regulators of cellular metabolism.[8] Mitochondria-associated lncRNAs, including both the RNAs derived from mtDNA and from nuclear-encoded lncRNAs that are transported into the mitochondria, may work in concert with transcription factors and other epigenetic regulators to modulate mitochondrial gene expression and mitochondrial function. These mitochondria-associated lncRNAs are important components of several gene regulatory networks,[9,10] potentially acting as epigenetic messengers to coordinate nuclear and mitochondrial functions.[11,12] Abnormal regulation of mitochondria-associated lncRNAs may lead to cell aging and oncogenesis.[10,13] Nuclear genome-encoded lncRNAs can function as "anterograde signals" to regulate mitochondrial function by hitching a ride with RNA transporters into mitochondria,[12] while mitochondrial genome-transcribed lncRNAs may shuttle via RNA transporters to the nucleus, where they can regulate the function of the nuclear genome, acting as a "retrograde signal." Using RNA fluorescence in situ hybridization (FISH) coupled with MitoTracker staining, we have recently shown that aberrant shuttling

Received 25 June 2020; accepted 30 September 2020;
https://doi.org/10.1016/j.omtn.2020.09.040.

Correspondence: Jiuwei Cui, MD, PhD, Key Laboratory of Organ Regeneration and Transplantation of Ministry of Education, Cancer Center, The First Hospital of Jilin University, 71 Xinmin Street, Changchun 130021, China.
E-mail: cuijw@jlu.edu.cn
Correspondence: Ji-Fan Hu, MD, PhD, Department of Medicine, PAVIR, Stanford University Medical School, VA Palo Alto Health Care System, Palo Alto, CA 94304, USA.
E-mail: jifan@stanford.edu; hujifan@jlu.edu.cn
Correspondence: Andrew R. Hoffman, MD, Department of Medicine, PAVIR, Stanford University Medical School, VA Palo Alto Health Care System, Palo Alto, CA 94304, USA.
E-mail: arhoffman@stanford.edu

of lncRNAs, whether nuclear genome-encoded or mitochondrial genome-transcribed, may play a critical role in abnormal mitochondrial metabolism in cancer cells.[14] For example, mitochondria genome-derived *lncND6* and *lncCytB* were enriched in the nucleus, while the nuclear genome-transcribed lncRNA *MALAT1* was found in the mitochondria of hepatocellular carcinoma cells. Therefore, lncRNAs may act as important messenger molecules linked to the regulation of both the nuclear and mitochondrial genomes.

In this study, we performed transcriptome sequencing to delineate the mitochondria-associated lncRNAs in HCC cells. We found that the nuclear genome-encoded lncRNA *MALAT1* was highly enriched in the mitochondria of HepG2 cells, supporting the hypothesis that *MALAT1* may act as an important factor in cancer metabolism reprogramming and mitochondrial function.[14] Although *MALAT1* is known to be involved in invasion and metastasis of numerous tumors,[15,16] its role in the regulation of cancer cell mitochondria has not been appreciated. We propose that *MALAT1* functions as a nuclear-mitochondrial epigenetic messenger to control metabolic reprogramming in HCC cells. Using the loss- and gain-of-function assays, we also explored the molecular mechanisms underlying the role of *MALAT1* in mitochondria in HCC.

RESULTS

Nuclear-Encoded lncRNA MALAT1 Is Aberrantly Enriched in the Mitochondria of Hepatoma Cells

To characterize regulatory components of metabolic reprogramming, we isolated mitochondria from hepatoma HepG2 cells (human hepatocellular carcinoma cell line) and normal hepatic HL7702 cells (human normal hepatocyte cell line). A modified protocol of the Mitochondria Isolation Kit was used to isolate mitochondria by avoiding contamination with nuclear RNAs. The isolated mitochondria were treated with RNase A prior to gradient purification. The quality of isolated mitochondria was assessed by quantitating the presence of small nuclear (snRNA) *U6* control (Figure S1). We detected enrichment of *MALAT1*, but not *U6*, in isolated mitochondrial RNAs.

After validating the quality of isolated mitochondria, we performed RNA transcriptome sequencing (RNA-seq) to identify the RNAs residing in mitochondria (Figure 1A). Using the criteria of >2 fold-change, $p < 0.05$, and the threshold of fragments per kilobase of transcript per million (FPKM) mapped reads >50, we identified a total of 246 RNAs that were differentially expressed between HepG2 and HL7702 cells (Figure 1B). We assessed the quality of the mitochondrial RNA-seq data by examining IGV reads for nuclear snRNAs *U6* and *U2*. As expected, we did not observe the presence of either *U6* or *U2* in the mitochondrial RNA-seq data (Figures S2B and S2C).

In addition to those lncRNAs that have previously been reported to be located within the mitochondria, including *RMRP*, *RPPH1*, and *RN7SK*,[12,17] we found that the nuclear genome-encoded *MALAT1* was enriched in the mitochondria of HepG2 cells (Figures S1, S2D, and S2E). Using qPCR, we also confirmed that mitochondrial *MALAT1* abundance was ~12-fold higher in hepatoma HepG2 cells than that in normal hepatic HL7702 cells. In addition, this nuclear-encoded lncRNA was also abundantly localized in the mitochondria of two other human hepatoma cell lines (Huh751 and SMMC-7721) (Figure 1C).

We then validated the presence of *MALAT1* lncRNA in the HepG2 mitochondria using RNA FISH. The location of mitochondria was tracked by a MitoTracker dye. Two types of fluorescence probes were used for RNA FISH. First, we used commercial fluorescent antisense oligonucleotide probes as provided in the Fluorescent In Situ Hybridization Kit (RiboBio, Guangzhou, China). We observed colocalization of *MALAT1* (red) and MitoTracker (green) in individual, snake-, and small fragment-like mitochondria (Figure 1D, enlarged panels). Second, we performed RNA FISH using digoxigenin-11-deoxyuridine triphosphate (DIG-11-dUTP)-labeled single-stranded DNA probes as prepared by asymmetric PCR.[14] We confirmed the colocalization of *MALAT1* (green) and MitoTracker (red) in individual mitochondria (Figure S3).Quantitation of RNA FISH also confirmed the localization of *MALAT1* in mitochondria (Figures 1E, 1F, S3B, and S3C). The *MALAT1*-mitoTracker merged area of each field was quantified using the ImageJ and Particle Analysis Plugin.[18,19] The quantitative co-localization was observed between *MALAT1* and mitochondria, with Rcoloc values of 0.73 ± 0.03 for commercial antisense oligonucleotide probes and 0.61 ± 0.12 for single-stranded DNA probes. As expected, the co-localization signal of *MALAT1* was decreased in cells that were transfected with shMALAT1 lentivirus (Figure S4).

To exclude the possibility that *MALAT1* is located in the cytoplasm itself or in some other cytoplasmic organelles, we isolated mitochondria and performed the RNA FISH assay for the isolated mitochondria on smearing slides. By combining the MitoTracker and probe staining, we validated the presence of *MALAT1* in the isolated mitochondria (Figure S5A, top panel). RNA FISH quantitation also confirmed the co-localization of *MALAT1* in isolated mitochondria, with Rcoloc values of 0.91 ± 0.03 (Figures S5B and S5C). Like *MALAT1*, the lncRNA *H19* is often overexpressed in HCC, and its dysregulation is closely related with tumorigenesis, metastasis, prognosis, and diagnosis.[20,21] However, *H19* was not found in the list of mtRNA-seq lncRNAs, and therefore we used *H19* as a lncRNA control. *H19* was not detected in isolated HepG2 mitochondria (Figure S5A, bottom panel). These data suggest that the nucleus-encoded lncRNA *MALAT1* can be transported to the mitochondria in HepG2 cells.

MALAT1 Binds to mtDNA and Alters Its Epigenotype

In the nucleus, *MALAT1* regulates multiple gene targets by altering epigenotypes where the lncRNA binds to DNA. For example, *MALAT1* controls the histone 3 lysine 4 (H3K4) epigenotype in the *EEF1A1* promoter.[22] To determine whether *MALAT1* utilizes a similar mechanism to regulate mitochondrial genes, we performed RNA reverse transcription-associated trap sequencing (RAT-seq)[23–25] to identify the specific *MALAT1*-mtDNA interaction sites and found that *MALAT1* interacted with multiple mtDNAs, including MT-RNR1, MT-RNR2, MT-CO2, MT-ND3, and MT-CYTB (Figure 2A, red arrows).

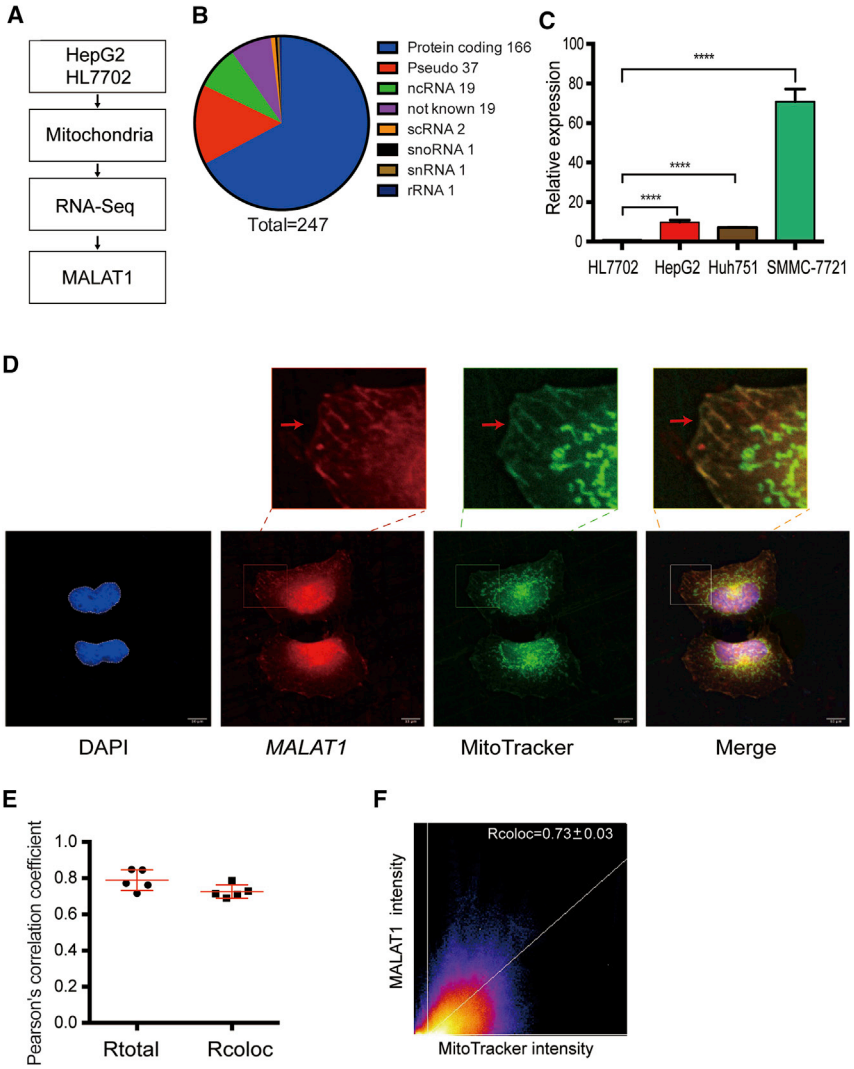

Figure 1. Nuclear lncRNA *MALAT1* Is Enriched in Mitochondria

(A) Identification of *MALAT1* as a mitochondria-associated lncRNA by mitochondrial RNA-seq. HepG2: HCC cells; HL7702: normal hepatic cells. (B) Distribution of 247 mitochondria-associated RNAs. (C) Differential enrichment of *MALAT1* in mitochondria comparing hepatoma HepG2 cells and normal hepatic HL7702 cells. *MALAT1* was quantitated by quantitative real-time PCR. The Ct value was normalized over that of *COX2* (mitochondrial housekeeping gene) and then standardized by setting normal HL7702 cells as 1 for comparison. ****$p < 0.0001$ between two cell lines. (D) RNA FISH of mitochondria-associated *MALAT1* in HepG2 cells. *MALAT1* was probed with antisense oligonucleotide probes (red) provided in the Ribo Fluorescent In Situ Hybridization Kit (C10910, RiboBio). Mitochondria were labeled with MitoTracker (green). Cells were counterstained with DAPI and imaged under a confocal laser-scanning microscope (Carl Zeiss). Scale bar = 10 μm. Note the colocalization of MALAT1 and MitoTracker in individual mitochondria (enlarged windows). (E) Quantitation of MALAT1 RNA FISH images. Pearson's correlation coefficient was calculated for the entire image (Rtotal) and the pixels above thresholds (Rcoloc) in 5 tested fields of view. (F) Scatterplot of *MALAT1* and MitoTracker. Channel 1 (red), *MALAT1*; channel 2 (green), MitoTracker. The regression line is plotted along with the threshold level for channel 1 (vertical line) and channel 2 (horizontal line). Mean ± SEM is indicated in the right upper corner of the image.

The *MALAT1*-mtDNA interaction was validated by a ChIRP assay (chromatin isolation by RNA purification). Mitochondria were isolated from HepG2 cells, and three 3′-end biotinylated oligonucleotide DNA probes were hybridized to *MALAT1*. The biotinylated probe/*MALAT1*/chromatin mtDNA complex was pulled down with streptavidin C1 beads, and mtDNA was quantitated by qPCR at the specific *MALAT1*-mtDNA interaction sites. This assay confirmed the binding of *MALAT1* to the mtDNA at the D-loop, *MT-CO2*, and *MT-ND3* sites (Figure 2B).

We recently reported that mitochondrial CpG DNA methylation changes during stem cell senescence.[26] In order to determine if the binding of *MALAT1* would alter the epigenotype at CpG islands of mtDNA, we used two short hairpin RNAs (shRNAs) to knock down *MALAT1* in HepG2 cells by targeting the middle and the 3′ fragment of *MALAT1* (Figure S6A).[22] CpG methylation was then examined by sodium bisulfite sequencing (Figure S6B). Mitochondrial CpG island 3 was predominantly unmethylated in HepG2 cells. After *MALAT1* knockdown, we observed increased DNA methylation at one CpG site of CpG island 3 (Figure S6C). The status of DNA methylation at CpG island 1, however, was not significantly affected by *MALAT1*.

We then determined if the binding of *MALAT1* would affect the transcription of mitochondrial genes. After *MALAT1* was knocked down using shRNA, we found decreased abundance of multiple mitochondrial genes, including *MT-CO1*, *MT-CO2*, *MT-ND5*, and *MT-ND3* (Figure 2C). Western blot analysis also showed reduction in the corresponding proteins (Figure 2D).

In order to determine if *MALAT1* regulates the morphology or number of mitochondria, we used transmission electron microscopy (TEM) and observed a reduction in mitochondria number in *MALAT1*-knockdown cells (Figure S7). The number of mitochondria was reduced by about half of the control cells (Figure 2E). As compared with the vector control (HepG2), the shRNA control group (shCT) also showed a slight reduction of mitochondrial number per cell (though not statistically different), suggesting that lentiviral infection itself may also have some effect on mitochondrial function.

We quantitated mitochondrial copy number by measuring DNA abundance from mitochondrial anterior, middle, and posterior

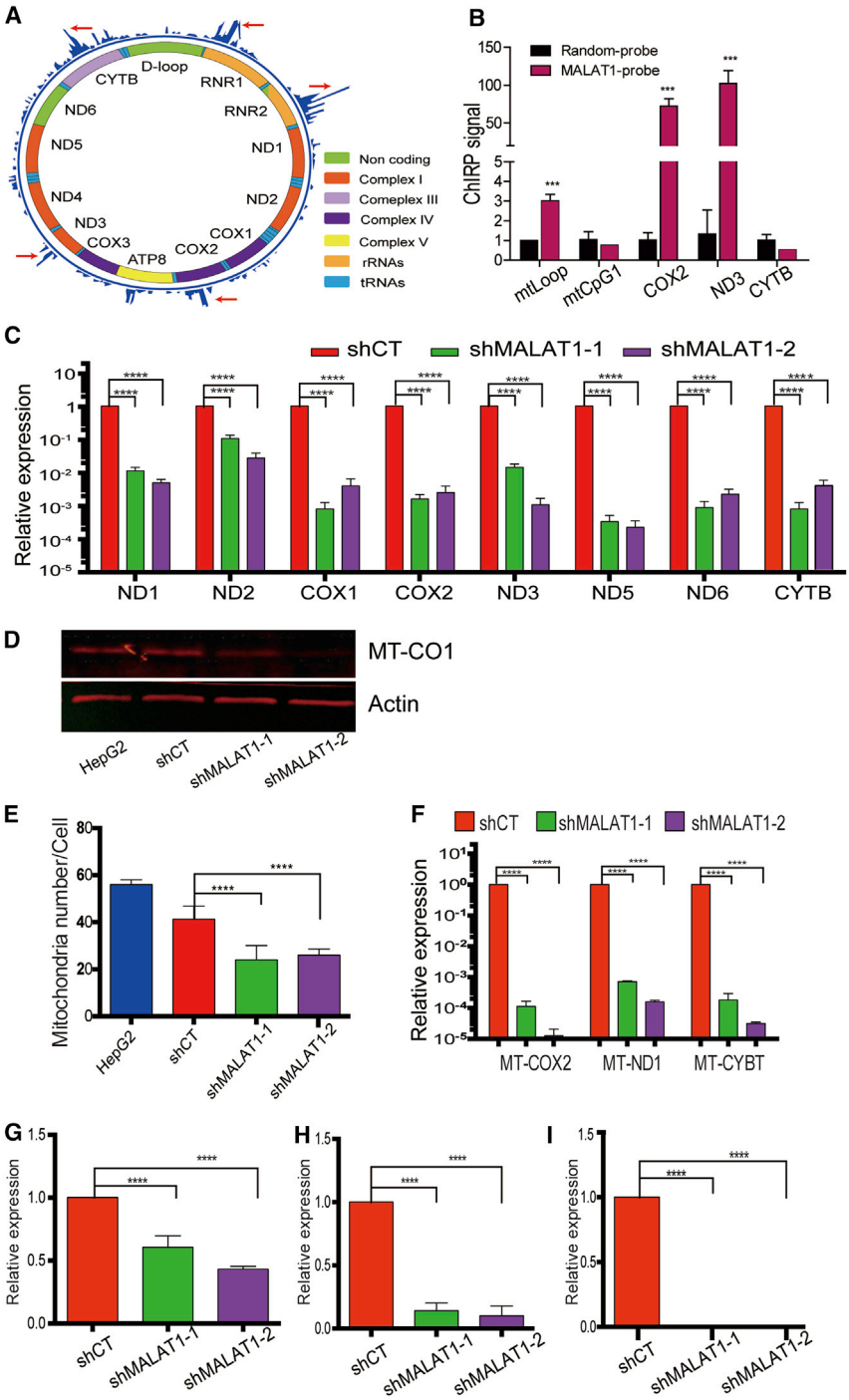

Figure 2. *MALAT1* Binds to mtDNAs and Affects Their Synthesis

(A) The binding of *MALAT1* to mtDNAs. RNA reverse transcription-associated trap sequencing (RAT-seq) was performed to find the *MALAT1*-interacting mtDNAs. The red arrows point to the *MALAT1* binding sites in the mitochondrial genome. (B) *MALAT1*-mtDNA interaction by ChIRP (chromatin isolation by RNA purification). Isolated mitochondria are cross-linked to fix the lncRNA-chromatin DNA complex. The lncRNA-interacting chromatin DNA is extracted, and the lncRNA-interacting target signal is quantitated by quantitative real-time PCR. For comparison, the Ct value was normalized over that of input and set the random probe control as 1. ***$p < 0.001$ as compared with the random control group. (C) The mtDNA transcriptome in *MALAT1* knockdown cells. The expression of each mitochondrial gene was quantitated by quantitative real-time PCR. Error bars represent the standard error of the average of three independent PCR reactions. Throughout the manuscript, the shCT group was set as 1 for comparison unless otherwise indicated. ****$p < 0.0001$ between the treatment and control groups. (D) Measurement of the mitochondrial proteome. Western blot was utilized to detect the expression of *MT-CO1* protein COX-1. (E) Mitochondria number. The number of mitochondria per cell was counted under transmission electron microscopy. n = 50 cells. ****$p < 0.0001$ between groups. (F) mtDNA copy number. The mtDNA copy number was quantitated by quantitative real-time PCR for three mtDNA genes (*ND1*, *CYB*, and *MT-CO2*). ****$p < 0.0001$ between groups. (G) Mitochondria. DNA replication factor SSBP1. The expression of SSBP1 was measured by quantitative real-time PCR. ****$p < 0.0001$ between groups. (H) mtDNA replication factor *PLOG1* by quantitative real-time PCR. ****$p < 0.0001$ between groups. (I) mtDNA replication factor *TFAM*. The expression of *TFAM* was measured by quantitative real-time PCR. ****$p < 0.0001$ between groups.

genes, including *MT-ND1*, *MT-CO2*, and *MT-CYB*. In agreement with the electron microscopy data, we found that mtDNA copy number was significantly decreased after *MALAT1* knockdown (Figure 2F).

mtDNA replication is independent of nuclear DNA replication, as mitochondria have their own replication complex.[27] PLOγ is a mammalian DNA polymerase that is present in mitochondria.[28] Mitochondrial single-stranded DNA-binding protein (*mtSSBP*) and Twinkle (*TWNK*) are mitochondrial helicases that work together to achieve helix destabilization during replication.[29] TFAM (mitochondrial transcription factor A) is an essential component of the nucleoid, which has been shown to be directly proportional to the mtDNA copy number.[30] We measured the expression of these mtDNA replication complex genes and found that all of these genes were significantly downregulated in shMALAT1-1/2 cells, in parallel with the decreased mtDNA copy number (Figures 2G–2I).

MALAT1 Is Essential for Mitochondrial Function in HepG2 Cells

Having shown that *MALAT1* affects mitochondrial number, we examined whether it participates in the regulation of mitochondrial biogenesis and energetics. *MALAT1* knockdown cells exhibited a reduction

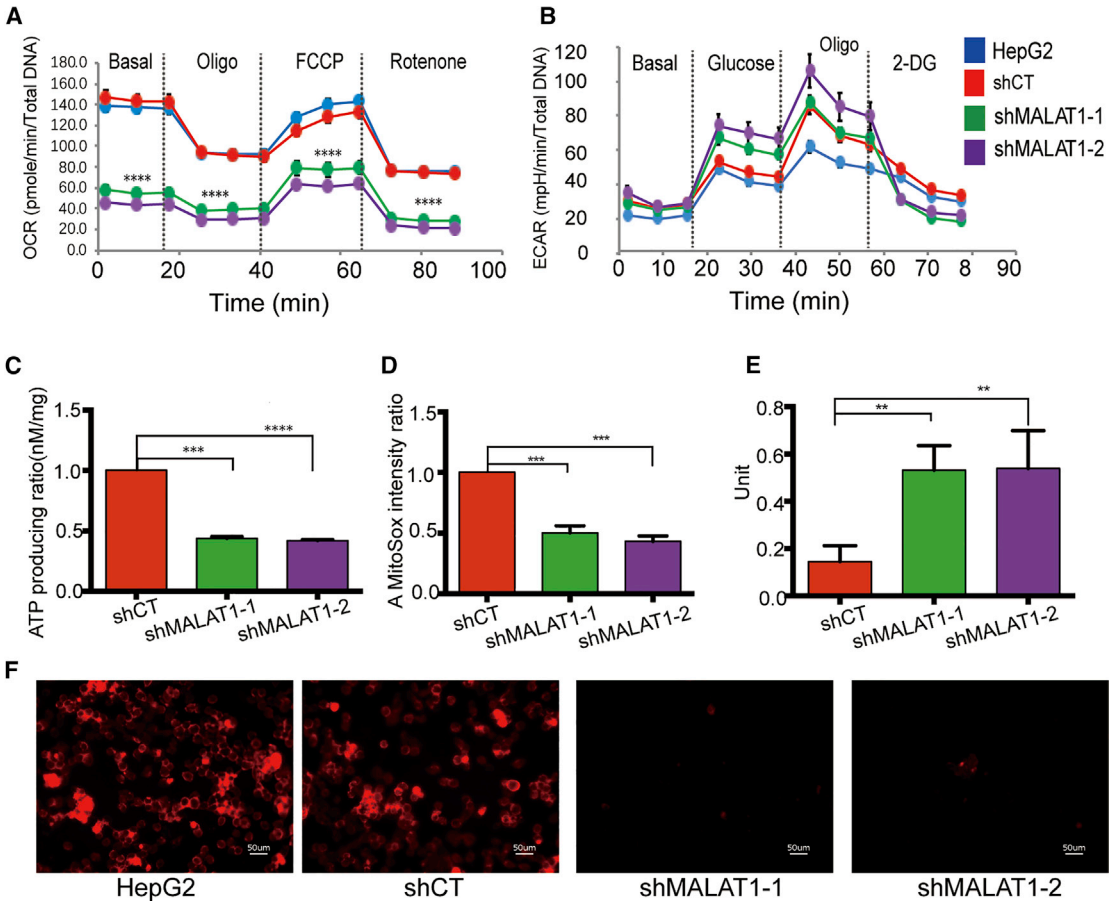

Figure 3. MALAT1 Knockdown Induces Mitochondrial Dysfunction

(A) *MALAT1* knockdown interferes with metabolic potentials in HepG2 cells. Metabolic potentials were assessed by measuring OCR. Treatment with shMALAT1-1 and shMALAT1-2 attenuated basal mitochondria respiration ability and relative OXPHOS ability. Data are presented as mean ± SEM from three independent assays. Significant differences were determined by one-way ANOVA followed by Tukey's post hoc test. ****$p < 0.001$ compared with the control groups. (B) Glycolytic function in *MALAT1* knockdown cells. Glycolytic function was assessed by measuring ECAR. No statistical differences were detected among the treatment groups. Data are presented as mean ± SEM from three independent assays. (C) *MALAT1* affects ATP production. The shMALAT1-1- and shMALAT1-2-treated cells show impaired ATP-producing ability compared with the control groups. (D) Fluorescence of the MitoSox-stained mitochondrial ROS. ****$p < 0.0001$, ordinary one-way ANOVA, followed by Student's t test. (E) Mitochondria Mn-SOD activities. **$p = 0.0016$, ordinary one-way ANOVA, followed by Student's t test. (F) Mitochondrial ROS production. Mitochondrial ROS showed red fluorescence by MitoSox staining. Scale bar = 50 μm. *MALAT1* knockdown cells show diminished ROS compared with control groups.

in four phases of the real-time oxygen consumption rate (OCR): basal respiration, ATP-producing capability, maximum respiration, and spare respiratory capacity decline. After *MALAT1* depletion, the basal respiration ability in HepG2 cells was reduced in comparison to that of the control cells (Figure 3A). However, there was no significant change in glycolytic function, as assessed by the extracellular acidification rate (ECAR) (Figure 3B). We then quantitated the mitochondria ATP-producing capability. *MALAT1* knockdown significantly decreased ATP synthesis as compared with the controls (Figure 3C).

Cancer cells have increased production of mitochondrial-derived reactive oxygen species (mROS), a byproduct of the mitochondrial electron transport chain that may lead to the activation of tumorigenic signaling and metabolic reprogramming.[31] We measured mROS using MitoSOX and found that mROS was significantly lower in the shMALAT1-1/2 cells than that in the control cells (Figures 3D and 3F). We also measured the activity of mitochondrial Mn-SOD, an antioxidative enzyme that eliminates mROS. We found that knocking down shMALAT1 significantly enhanced its specific enzymatic activity in the mitochondria (Figure 3E).

Enrichment of MALAT1 Affects Mitochondrial Apoptosis

Mitochondria apoptosis was increased in shMALAT1-treated HepG2 cells, where we observed swollen mitochondria, enlarged vesicular matrix compartments, small vesicular matrix compartments surrounding swollen vesicular compartments, and an absent inner boundary membrane (Figure 4A). In some mitochondria, two lamellar cristae were contained within a swollen matrix bound by

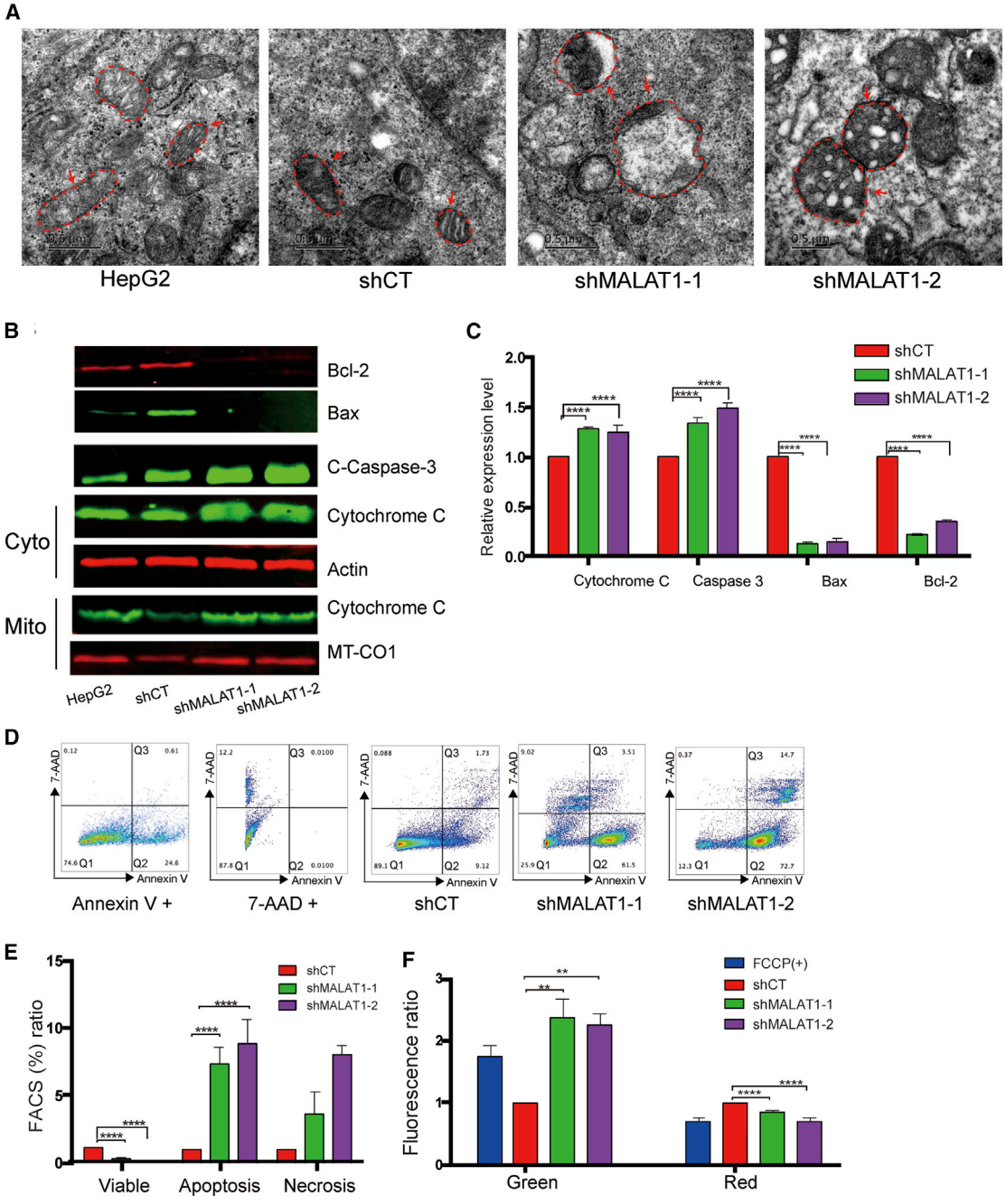

Figure 4. Knockdown of *MALAT1* Induces Mitochondrial Apoptosis

(A) Abnormal mitochondrial structure in *MALAT1* knockdown HepG2 cells. Scale bar = 0.5 μm. Under TEM, mitochondria had swollen vesicular matrix compartments and small vesicular matrix compartments surrounding a swollen vesicular compartment. (B) Mitochondria apoptosis biomarkers. Western blot was used to measure the biomarkers for mitochondrial apoptosis, including Bcl-2, Bax, Caspase-3, and cytochrome C. β-Actin and *MT-CO1* were used as the cytoplasmic and mitochondrial controls. (C) Quantitation of western blot results. Data are presented as mean ± SEM. Significant differences were determined by one-way ANOVA followed by Student's t test. ****$p < 0.001$ compared with the shCT group. (D) FACS analysis of cell death. Standard dot plot diagram from FACS shows the progression of cell death. Q1, double negative (annexin V and 7-AAD negative) represented healthy cells; Q2, annexin V positive and 7-AAD negative represented apoptotic cells; Q3, annexin V &7-AAD double positive represented necrotic cells. (E) Percentage of cell population. Apoptotic, healthy, and necrotic cells were quantitated by flow cytometry. ****$p < 0.0001$ compared with the shCT control group. (F) Mitochondria membrane potential. The membrane potential was measured by JC-1 staining. FCCP was used as the positive control of cell apoptosis. In cells with high mitochondrial membrane potential, JC-1 spontaneously forms complexes with intense red fluorescence. In apoptotic or unhealthy cells, JC-1 was stained with green fluorescence. The ratio of green to red fluorescence is associated with the membrane potential. ****$p < 0.0001$, **$p < 0.01$ compared with the shCT control group.

an inner boundary membrane, and the outer membrane appeared to be ruptured. However, some differences in mitochondrial morphology were noticed between the two shRNA-treated groups. In the shMALAT1-1 group, mitochondria had an expanded matrix space with less dense staining of the matrix and fewer cristae, and the outer membrane was ruptured by the expanded matrix. However, the shMALAT1-2 group exhibited less severe apoptosis.

As seen in Figures 4B and 4C, *MALAT1* knockdown induced a series of events related to mitochondrial apoptosis, including caspase-3 activation, increased expression of cytochrome C, and attenuated expression of *Bcl-2*. The mitochondrial apoptosis activator *BAX* was downregulated in shMALAT1-treated cells, suggesting that shMALAT1-induced apoptosis may not be derived from the formation of an activated BAX oligomeric pore.[32] Again, we also observed some variations in apoptosis markers between the HepG2 and shCT controls. It is likely that the lentiviral infection itself may have some effect on these variables.

Apoptotic cells were further quantitated using Annexin V/7-AAD fluorescence-activated cell sorting (FACS) staining (Figures 4D and 4E). Standard dot plot diagrams from FACS illustrate the progression of cell death (Figure 4D). Q1, Q2, and Q3 represented healthy, apoptotic, and necrotic cells, respectively. We found that *MALAT1* knockdown induced apoptosis in HepG2 cells. These findings demonstrate that *MALAT1* is required for maintaining normal mitochondrial function by suppressing mitochondria-specific apoptosis.

We also measured mitochondria membrane potential using JC-1 staining (Figure 4F). JC-1 green fluorescence indicates a decrease in mitochondrial membrane potential, an early event in apoptosis. FCCP (carbonylcyanide p-(trifluoromethoxy) phenylhydrazone) was used as the positive control for cell apoptosis. We showed that *MALAT1* knockdown increased the loss of mitochondrial membrane potential, confirming that knockdown of *MALAT1* in HepG2 triggers an early event in apoptosis.

MALAT1 Functions via the Mitochondrial Autophagy Pathway

Damaged mitochondria are normally removed by a specialized autophagy process, called mitophagy. Selective autophagy targets different groups of substrates and damaged organelles for autophagosome-lysosomal degradation.[33,34] Several pathways are activated in mitophagy. In the PINK1/Parkin pathway, phosphorylation of Parkin and binding to phosphorylated-ubiquitinated proteins result in the accumulation of ubiquitinated chains on a variety of mitochondrial proteins, which are recognized by selective cargo receptors, including SQSTM1/p62, Optineurin, and NDP52.[35,36] In the BNIP3L/Nix pathway, BNIP3 and BNIP3L/Nix bind to members of the LC3 family to target mitochondria to autophagosomes. We were interested to learn whether mitochondrial *MALAT1* might be involved in the regulation of this mitophagy pathway.

We used western blot to measure these mitophagy pathway proteins. shMALAT1-treated cells exhibited a significant decrease in mitophagy events. Compared with the control cells, *MALAT1* knockdown cells showed reduced expression of mitophagy markers, particularly PINK1, SQSTM1/p62, NDP52, BNIP3, and LC3B-I/II (Figures 5A and 5B).

Microtubule-associated protein 1 light chain 3 (LC3) plays a critical role in autophagy. The LC3B II/I ratio, designated the cytosolic LC3 ratio, reflects the total proteolytic flux and is a sensitive quantitative index to monitor autophagy in the cell. The LC3B-II/I ratio increases when autophagy is induced. After *MALAT1* knockdown, the LC3B-II/I ratio was significantly decreased (Figure 5C), suggesting the critical role of *MALAT1* in this autophagy process.

We also examined mitochondria and lysosomal surface markers. There was a decrease in the mitochondria outer membrane marker Cyclophilin F (CYDP) and an increase in the lysosome-associated membrane glycoprotein (LAMP-1) (Figures S8A and S8B). Lysosomal enzymes function optimally in an acidic environment, and increases in lysosomal pH can impede enzymatic ability. We labeled lysosomes using lysotracker and found that the number of red-stained (acidic) lysosomes decreased significantly in the *MALAT1*-treated cells compared with the control group cells (Figures 5D and S8C), suggesting impairment of lysosomal function in *MALAT1*-deficient cells.

Effect of MALAT1 on the Biological Behavior of Hepatocellular Carcinoma Cells

MALAT1 is associated with lung carcinoma invasion and metastasis. We examined the invasion of shMALAT1-1/2 cells using Transwell assays and found that the average number of invading *MALAT1* knockdown cells was significantly lower than that from HepG2 random vector cells (shCT) (Figure 6A). Similarly, *MALAT1* knockdown also altered cell proliferation (Figure 6B), wound healing (Figure 6C), progression through the cell cycle (Figure S9A), and clone formation (Figure S9B).

In an initial step to examine the shuttling of nuclear *MALAT1* to mitochondria, we isolated mitochondria from HepG2 cells and performed RNA chromatin precipitation (RNA immunoprecipitation [RIP]) for HuR[12,37,38] and MTCH2 (mitochondrial carrier homolog 2).[39–41] *MALAT1* interacted with MTCH2 both in the whole cell (Figure S10A) and in isolated mitochondria (Figure S10B). *MALAT1* also interacted with HuR (Figure S10C). These data suggest that *MALAT1* may be shuttled by the HuR and MTCH2 complexes into mitochondria, where *MALAT1* regulates metabolism and apoptosis (Figure 6D).

DISCUSSION

MALAT1, a highly conserved lncRNA, exerts an oncogenic role in multiple cancers, including HCC. Previous work has mainly focused on the role of *MALAT1* in metastasis, prognosis, and tumorigenesis,[15,42] but its role in mitochondrial dysfunction and aberrant energy metabolism has not been examined. In this study, we provide the first evidence that in hepatoma HepG2 cells, the nuclear

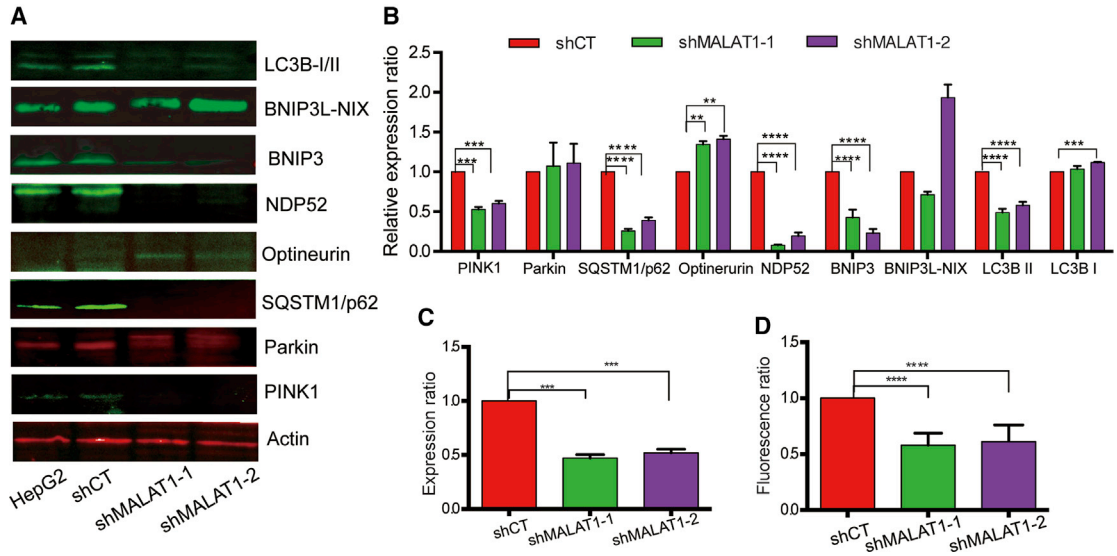

Figure 5. *MALAT1* Knockdown Impairs Mitophagy

(A) Mitophagy biomarkers were detected by western blot. β-Actin was used as the control. (B) Quantitation of mitophagy biomarker western blot results. ****$p < 0.0001$, **$p < 0.01$ compared with the shCT control group. (C) The LC3B II/I ratio. Autophagy was assessed by LC3B-II/I ratio. After knockdown of *MALAT1*, the LC3B-II/I ratio was significantly decreased. ****$p < 0.0001$ compared with the shCT control group. (D) Acidic lysosome by Lysotracker staining. The intensity of the fluorescence stained by lysotracker was measured. ****$p < 0.0001$ compared with the shCT control group.

genome-encoded lncRNA *MALAT1* is aberrantly transported to the mitochondria, where it plays a pivotal role in regulating mitochondrial function. *MALAT1* binds to multiple loci on mtDNA, where it epigenetically regulates mitochondrial function. Knockdown of *MALAT1* induces alterations in the structure, transcriptome, and function of mitochondria. *MALAT1*-deficient cells show multiple abnormalities in mitochondrial function, including mitochondrial copy number, oxidative phosphorylation (OXPHOS), ATP production, mitophagy, and apoptosis. This study suggests that the nuclear genome-encoded lncRNA *MALAT1* may function as an epigenetic factor in the regulation of mitochondrial metabolism in HCC cells (Figure 6D).

The mitochondrial genome consists of 16,569 base pairs of DNA that encode 37 genes to synthesize core subunits of the oxidative phosphorylation system.[43,44] The mitochondrial genome, however, cannot independently produce all of the protein components needed for energy metabolism. Instead, mitochondria rely heavily on imported proteins, and perhaps RNAs, encoded by the nuclear genome.[9,10] Here, we provide the first evidence that *MALAT1* lncRNA may function as an epigenetic messenger to coordinate a variety of functions between the nucleus and the mitochondria. *MALAT1* does not encode a protein, but it is able to bind to mtDNAs and epigenetically regulate mitochondrial function. Inhibition of this *MALAT1*-mediated communication network interrupts the function of mitochondria, including mitochondrial biosynthesis and energy metabolism. In addition, *MALAT1* knockdown stimulates mitochondrial apoptosis and suppresses mitophagy. Recently, we also demonstrated that *lncCytB*, a mitochondrial genome-encoded lncRNA, can be aberrantly transported into the nucleus in HepG2 cells.[22] Clearly, there is significant crosstalk between the nucleus and mitochondria that can modify cancer cell metabolism.[9,45] Shuttled lncRNAs, such as the nuclear genome-encoded *MALAT1* and the mitochondrial genome-encoded lncCytB, may function as essential molecules to deliver epigenetic signals to tightly coordinate mitochondrial and nuclear function.[9,10]

MALAT1 was first identified as an oncogenic lncRNA in association with the survival and metastasis of non-small-cell lung cancer. Recent studies have also associated its expression with the survival and progression of multiple malignancies, including uterine endometrial stromal sarcoma, breast cancer, and HCC.[46,47] Although its association with clinical outcomes has been well studied, its mechanism of action has not been well characterized. Several studies have been focused on its role as a competing endogenous RNA (ceRNA) to regulate microRNAs (miRNAs), including miR-195, miR-183, miR-23c, miR-155, miR-197, miR-203, and miR-20b-5p. Our data reveal a novel mechanism for *MALAT1* action in cancer. In the mitochondria, *MALAT1* regulates energy metabolism, mtDNA replication, transcription, mitochondrial apoptosis, mitophagy, and mitochondria stability.

Autophagy (macroautophagy) is a fundamental cellular process that helps cells maintain the metabolic state to afford high-efficiency energy requirements.[48] Autophagy targets damaged intracellular organelles and misfolded proteins to the lysosome for degradation. Mitophagy, a special form of autophagy, plays a critical role in the removal of damaged mitochondria and in the control of mitochondria

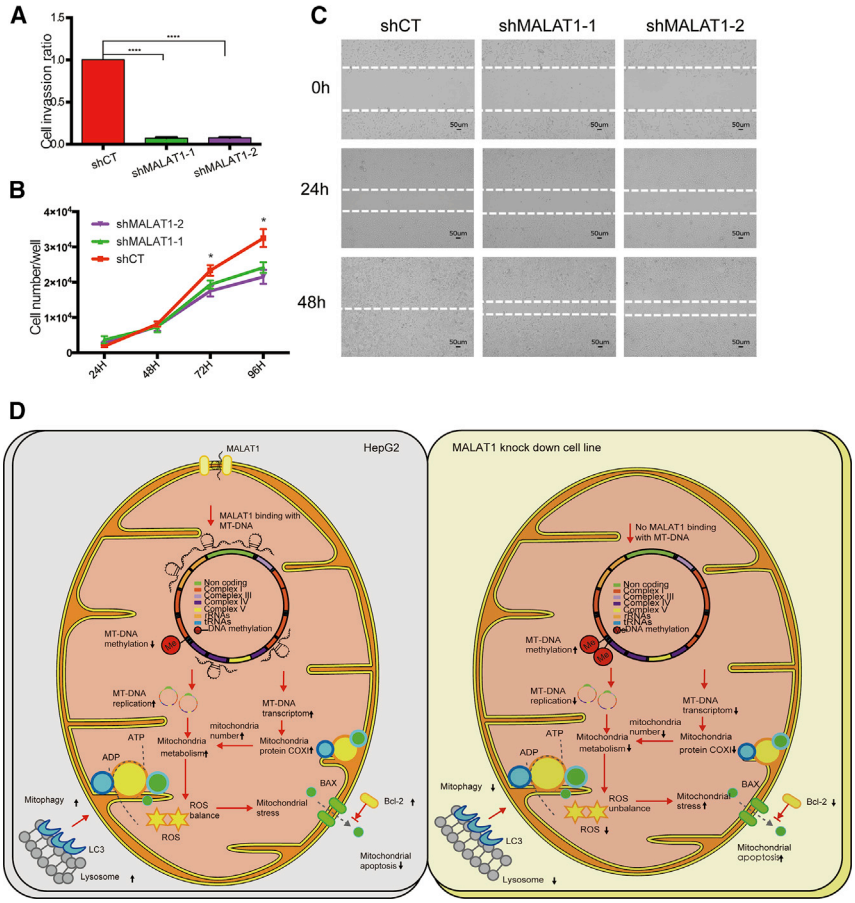

Figure 6. *MALAT1* Affects Cancer Biology Behavior

(A) *MALAT1* knockdown cells showed decreased cell invasion ability. Ordinary one-way ANOVA, followed by Student's t test. ****p < 0.0001 compared with the shCT control group. (B) Cell proliferation assay. Total cells were counted after 24 h, 48 h, 72 h, and 96 h. Ordinary one-way ANOVA, followed by Student's t test. ****p < 0.0001 compared with the shCT control group. (C) Wound healing assay. Scale bar = 50 μm. MALAT1 knockdown cells showed slower wound healing capability indicating slower migration ability. (D) The putative model of *MALAT1* as an epigenetic messenger in controlling cancer metabolism. *MALAT1* is aberrantly expressed in HCC mitochondria, where it binds to mtDNA and alters mtDNA methylation and mitochondrial function, including mitochondria synthesis, metabolism, mitophagy, ROS regulation, and apoptosis.

quality.[49,50] Autophagy facilitates metastasis in HCC by upregulating the expression of epithelial-mesenchymal transition (EMT).[51] In this study, we demonstrate that *MALAT1*-deficient cells exhibit decreased expression of the mitophagy markers PINK1, SQSTM1/p62, NDP52, BNIP3, and the LC3B-II/I ratio. By labeling lysosomes using LysoTracker, we show that the number of red-stained lysosomes was reduced in the shMALAT1-treated cells, suggesting that *MALAT1* plays a critical role in the regulation of autophagy in hepatoma cells.

The data from this study indicate that, in addition to its regulatory role at the transcriptional and/or post-transcriptional levels, *MALAT1* may act as a nucleus-to-mitochondria messenger. *MALAT1* is aberrantly expressed in HCC cells. After being transported into mitochondria, *MALAT1* binds to multiple sites of mtDNA and alters the status of DNA methylation at the CpG 3 site in front of *MTCO1*. Both quantitative real-time PCR and western blot assays document the downregulation of COX1 in *MALAT1* knockdown cells. Mitochondrial metabolism is also altered in these cells. Our results thus support the concept that retrograde and anterograde signaling occur as lncRNAs shuttle between the nucleus and mitochondria.[9,10] As a result of this crosstalk, lncRNAs function as epigenetic messengers, altering mitochondrial metabolism during oncogenesis. Mitochondria-derived lncRNAs, on the other hand, may also shuttle into the nucleus, where they may regulate target genes related to tumor phenotypes.[22]

Dysregulation of cellular energetics is a hallmark of cancer cells, with enhanced absorption and utilization of glucose and glutamine. lncRNAs are implicated in the regulation of this metabolic reprogramming. For example, glutamine metabolism and ROS, the most important by-products of the electron transport chain in the mitochondria, are regulated by lncRNAs *HOTTIP*,[52] *CCAT2*,[53] and *UCA1*.[54] lncRNAs *Ftx* and *p21* promote the Warburg effect and enhance tumor progression.[55,56] *HOTAIR* decreased UQCRQ (Ubiquinol-Cytochrome C Reductase, Complex III Subunit VII), leading to the impairment of the mitochondrial respiratory chain.[57] *SAMMSON* interacted with mitochondrial surface protein P32 in cancer cells.[58,59] Nuclear *MALAT1* mediated glycolysis through the HIF-1α pathway in HCC.[60] In this study, we show that *MALAT1* functions as a nucleus-to-mitochondria epigenetic messenger to control metabolic reprogramming. *MALAT1* binds to mtDNA and regulates mitochondrial genes epigenetically. Knockdown of *MALAT1* induces multiple abnormalities in mitochondrial function, including altered mitochondrial structure, low OXPHOS, decreased ATP production, reduced mitophagy, decreased mtDNA copy number, and activation of mitochondrial apoptosis.

Overall, this study greatly expands our knowledge of the nucleus-encoded oncogenic lncRNA *MALAT1* in regulating mitochondrial function. We provide the first evidence that the nuclear genome-encoded lncRNA *MALAT1* functions as a critical epigenetic player in the regulation of mitochondrial metabolism of hepatoma cells, laying the foundation for further clarifying the roles of lncRNAs in tumor metabolic reprogramming. Additionally, this study provides solid evidence that lncRNA may function as an epigenetic messenger to coordinate a variety of functions between the nucleus and the mitochondria.

It is possible that knocking down *MALAT1* using shRNAs may not target *MALAT1* specifically in mitochondria. Future studies are necessary to target *MALAT1* using other approaches, like antisense LNA GapmeRs and CRISPR Cas9. Ideally, it would be preferable to target the lncRNA specifically in mitochondria, while preserving the nuclear *MALAT1*. An unbiased global gene expression profile could then be used to evaluate the effect on pathways related to mitochondria, autophagy, and apoptosis.

We have demonstrated that the nuclear-encoded *MALAT1* can be shuttled to mitochondria by RNA-binding proteins HuR and MTCH2. Perhaps a post-transcriptional modification, like m6A, might act as a signal that regulates the mitochondrial translocation of the nuclear *MALAT1*. Finally, *MALAT1* may also function as a precursor and produce a highly conserved, tRNA-like 61 bp cytoplasmic RNA (MALAT1-associated small cytoplasmic RNA, *MASCRNA*).[61] It would be interesting to learn if this small tRNA-like cytoplasmic RNA is also shuttled into mitochondria.

In conclusion, the lncRNA *MALAT1* is a nucleus-to-mitochondria epigenetic messenger that influences metabolic reprogramming in HCC cells by regulating mitochondrial function in cancer cells.

MATERIALS AND METHODS

Cell Culture

HepG2 cells and 293T cells, purchased from ATCC, were maintained in high-glucose DMEM media supplemented with 10% fetal bovine serum (FBS) and 1% penicillin/streptomycin. The normal hepatic cell line HL7702 was purchased from the Type Culture Collection of the Chinese Academy of Sciences (Shanghai, China) and was maintained with 20% FBS and 1% penicillin/streptomycin in high-glucose DMEM media at 37°C with 5% CO_2.

Mitochondria Isolation, Reverse Transcription, and RNA Sequencing

Mitochondria were isolated using a Qproteome Mitochondria Isolation Kit (QIAGEN, Cat.#37612) with modifications as previously described.[62,63] Specifically, the combined mitochondria supernatants were treated with RNase A buffer (4 μg/mL RNase A) at room temperature for 15 min to remove any cytoplasmic RNA on the outer mitochondrial membranes. After centrifugation at 6,000×*g* for 10 min, the pellet was suspended in Mitochondria Purification Buffer and was subjected to gradient purification following the manufacturer's manual.

The isolated mitochondria and whole-cell lysate were used for RNA extraction using Trizol (Invitrogen, CA, USA). To confirm the purity of the isolated mitochondria, mitochondrial RNAs were reverse transcribed into cDNAs, and qPCR was performed to quantitate the mitochondria genome-encoded RNA (*COX2*) and the nuclear RNA (*U6*). Mitochondrial RNAs were then subjected to Illumina sequencing (Shanghai Biotechnology, Shanghai, China).

Quantitation of Gene Expression by Quantitative Real-Time PCR

Whole-cell and mitochondrial cDNAs were synthesized, and quantitative real-time PCR was performed using the FastStart Universal SYBR Green Master mix (Millipore Sigma, MA, USA) with a StepOnePlus real-time PCR system (ABI Prism 7900HT; Applied Biosystems, USA). The threshold cycle (Ct) values of target genes were normalized over the Ct of *COX2* for gene expressions in mitochondria and the Ct of β-actin in whole cell lysate. For comparison, the shCT group was set as 1 unless otherwise indicated. Primers used for real-time PCR and quantitative real-time PCR are listed in Table S1.

Western Blot for Mitochondrial Proteins

Western blot was used to detect mitochondrial proteins. Antibodies used for western blot were: Anti-LAMP1 antibody-Lysosome Marker (ab24170), Anti-Cyclophilin F antibody (ab110324), Mitophagy Antibody Sampler Kit (Cell Signaling Technology [CST], #43110), Bcl-2 (124) Mouse monoclonal antibody (mAb) (CST, #15071), Cytochrome *c* (D18C7) Rabbit mAb (CST, #11940), Caspase-3 antibody (CST, #9662), Bax (D2E11) Rabbit mAb (CST, #5023), β-Actin (8H10D10) Mouse mAb (CST, #3700), and BID antibody (CST, #2002). The blots were developed by Odyssey clx Imaging System (LI-COR).

Knockdown of MALAT1 in HepG2 Cells

To study the role of *MALAT1* in HCC cells, two shRNAs were cloned into a pGreenPuro vector to knockdown *MALAT1*: shMALT1-1#: 5′-CACAGGGAAAGCGAGTGGTTGGTAA-3′ and shMALAT1-2#: 5′-GATCCATAATCGGTTTCAAGGTA-3′. The copGFP reporter in the vector was used to track the lentiviral transfection. A random shRNA (5′-GCAGCAACTGGACACGTGATCTTAA-3′) was cloned in the same vector as the assay control (shCT). Three days after lentiviral infection, HepG2 cells were selected by puromycin, and mixed stable cells were collected for gene analysis by RT-PCR.

RAT-Seq

An RNA RAT-seq assay[64] was used to examine lncRNA-mtDNA interactions. After *in situ* reverse transcription in the isolated nuclei using gene strand-specific reverse transcription and biotin-dCTP (deoxycytidine triphosphate), the biotin-cDNA/chromatin DNA complex was isolated with streptavidin magic beads (Invitrogen, CA, USA) and used for PCR amplification of the genomic DNA that interacts with the lncRNA.

RNA FISH Assay

FISH was performed using two probes. In the first approach, we performed RNA FISH for *MALAT1* using commercial antisense oligonucleotide probes in a FISH Kit (C10910, RiboBio, China). Briefly, cells were fixed in 4% formaldehyde for 10 min and were permeabilized in 1 × PBS containing 0.5% Triton X-100 for 5 min at 4°C. After treatment with pre-hybridization buffer at 37°C for 30 min, hybridization was carried out with fluorescent probes following the protocol provided by the manufacturer. Images were obtained using a confocal laser-scanning microscope (Carl Zeiss).

In a second approach, RNA FISH was performed using asymmetric PCR-derived antisense DNA probes.[14] FISH probes are prepared as antisense single-stranded DNA molecules using a simple asymmetric

PCR and labeled with digoxigenin-labeled dUTP (Digoxigenin labeling DNA mix, Cat.11277065910 ROCHE). After probe hybridization, lncRNAs in the mitochondria are detected by anti-digoxigenin-fluorescein. For RNA FISH of the isolated mitochondria smear, we first treated mitochondria supernatants with RNase A buffer (4 μg/mL RNase A) at room temperature for 15 min to remove the cytoplasmic RNA on the outer mitochondrial membranes. After centrifugation, mitochondria were smeared on slides for RNA FISH. In combination with MitoTracker (MitoTracker Red CMXRos, Cat.M7512, Invitrogen), RNAs can be visualized within mitochondria. The locations of *MALAT1* FISH probes are shown in Figure S11.

ChIRP

Mitochondria were first isolated following the Qproteome Mitochondria Isolation Kit (QIAGEN, Cat. #37612) manual. After treatment with RNase (4 μg/mL RNase A), the isolated mitochondria were cross-linked, lysed, and sonicated. Three 3′-end biotinylated oligonucleotide DNA probes were hybridized to *MALAT1*. The biotinylated probe/*MALAT1*/chromatin mtDNA complex was pulled down with streptavidin C1 beads (Invitrogen 65002). The *MALAT1*-pulldown chromatin mtDNA was extracted and quantitated by qPCR for the interacted mtDNA.[24]

Mitochondrial Oxidative Phosphorylation and Glycolysis

Mitochondrial metabolism was determined by measuring the OCR and ECAR of the cells with the XF-96 Flux Analyzer (Seahorse Biosciences, North Billerica, MA, USA) at the Gerontology Seahorse Core Facility.[65] Seahorse XF Cell Mito Stress Test and Glycolysis Stress Test were used to examine OCR and ECAR, respectively, following the manufacturer's instructions. All readings were normalized to total DNA content.

Detection of mtDNA Copy Number

mtDNA copy number was examined using a previous protocol.[65] Briefly, genomic DNA was extracted from 300,000 cells by phenol-chloroform extraction. The mitochondrial copy number was estimated by real-time PCR (CFX Connect Real-Time System, Bio-Rad) using three mtDNA targets (*ND1*, *CYB*, and *MT-CO2*) and one cytoplasmic DNA target (β-actin) (Integrated DNA Technologies [IDT], CA, USA).

Detection of mtDNA Methylation

mtDNA methylation was measured as previously described.[26,42] The PCR primers used to amplify the bisulfite-treated mtDNA are listed in Table S1. PCR products were cloned into the pJet vector and sequenced for the quantitation of CpG methylation. DNA methylation was calculated as the average percentage of all CpG sites.

Transmission Electron Microscopy

Transmission electron microscopy was used to examine structural changes of mitochondria. Control and shMALAT1-treated HepG2 cells were pre-fixed with 4% glutaraldehyde and then fixed with 1% citric acid. Samples were dehydrated with ethanol, embedded with Eponate 12 epoxy resin, and semi-thin sliced by LEICA EM UC7 Ultra-Thin Slicer. After double staining with uranyl acetate and lead citrate, slides were observed under transmission electron microscopy (FEI Tecnai Spirit). For mitochondrial number quantitation, electron microscope slides were viewed and counted by two independent technicians. In each group, 3 cells (N = 3) were counted for the number of mitochondria in the treatment group.

Detection of mROS, Mitochondrial SOD Enzyme Activity, and JC-1 Mitochondria Membrane Potential

mROS was detected by MitoSOX (M36008), following the manufacturer's instructions. Plasma superoxide dismutase (SOD) activity was detected using a Cu/Zn-SOD and Mn-SOD Assay Kit (S0103) from Beyotime Institute of Biotechnology (Beijing, China) according to manufacturer's protocol.[8] Mitochondrial membrane potential was detected by the JC-1 kit (C2006) from Beyotime Institute of Biotechnology (Beijing, China), following the manufacturer's protocol.

RIP

The Magna RIP RNA-Binding Protein Immunoprecipitation Kit (EMD Millipore, #17-700) was used to assess the interaction of the lncRNA with MTCH2/HuR following the manufacturer's specifications.[66] Rabbit anti-IgG was used as the RIP control. We used ΔCt values for determining enrichment fold change relative to IgG controls.

Cell Cycle and Apoptosis Analysis by Flow Cytometry

Cells were fixed in absolute ethyl alcohol at −20°C overnight, washed twice with PBS, and resuspended in PI staining solution containing 0.1 mg/mL RNase A, 50 μg/mL propidium-iodide, and 0.2% Triton. Cell cycle distribution was analyzed using bivariate flow cytometry on a Fortessa flow cytometer. To detect cell apoptosis, 2×10^5 cells were harvested, and then resuspended in 500 μL Annexin V binding buffer, and incubated with 5 μL Annexin V for 10 min and 5 μL 7-AAD for 15 min, following the manufacture's instruction by flow cytometry.

Statistical Analysis

The data are expressed as mean ± standard deviation of at least three sample replicates, unless stated otherwise. For comparison, the value of the random shRNA control group (shCT) was set as 1, and the fold-change was calculated for the shMALAT1-1/shMALAT1-2 groups. Data were analyzed using GraphPad software (version 6.0c; PRISM, San Diego, CA, USA). Student's t test or one-way ANOVA (Bonferroni test) was used to compare statistical differences for variables among treatment groups.

Results were considered statistically significant at $p < 0.05$.

Availability of Data and Material

Raw FASTQ sequencing files comprised of three cell mitochondrial RNA datasets have been deposited to the NCBI Gene Expression Omnibus under accession number GEO: GSE119946.

SUPPLEMENTAL INFORMATION

Supplemental Information can be found online at https://doi.org/10.1016/j.omtn.2020.09.040.

AUTHOR CONTRIBUTIONS

Conception and design: A.R.H., J.F.H., and J.C.; Development of methodology: Y.Z., L.Z., X.L., and P.C.; Acquisition of data: Y. Z., X.L., S.K., J.X., L.Z., H.L., T.S., and X.W.; Analysis and interpretation of data: Y.Z., X.L., S.J.K., J.X., L.Z., H.L., T.S., and X.W.; Writing, review, and/or revision of the manuscript: Y.Z., A.R.H., J.F.H., and J.C.; Administrative, technical, or material support (i.e., reporting or organizing data, constructing databases): L.L., S.Z., W.L., Y.M., Y.L., M.L., and S.L.; Study supervision: A.R.H., J.F.H., and J.C.

CONFLICTS OF INTEREST

The authors declare no competing interests.

ACKNOWLEDGMENTS

This work was supported by a Key Project of Chinese Ministry of Education grant (311015), the National Basic Research Program of China (973 Program; 2015CB943303), a Nation Key Research and Development Program of China grant (2016YFC13038000), the Research on Chronic Noncommunicable Diseases Prevention and Control of National Ministry of Science and Technology (2016YFC1303804), the National Health Development Planning Commission Major Disease Prevention and Control of Science and Technology Plan of Action, Cancer Prevention and Control (ZX-07-C2016004), the National Key R&D Program of China (2018YFA0106902), the National Natural Science Foundation of China (82050003, 32000431, 31430021, 81874052, 81672275, 31871297, and 81670143), the Natural Science Foundation of Jilin Province (20150101176JC, 20180101117JC, and 20130413010GH), the Provincial Science Fund of Jilin Province Development and Reform Commission (2014N147 and 2017C022), and a California Institute of Regenerative Medicine (CIRM) grant (RT2-01942). This work was supported in part by a Merit Review from the United States Department of Veterans Affairs, Biomedical Laboratory Research and Development Service (BX002905).

REFERENCES

1. Zong, W.X., Rabinowitz, J.D., and White, E. (2016). Mitochondria and Cancer. Mol. Cell *61*, 667–676.
2. Vyas, S., Zaganjor, E., and Haigis, M.C. (2016). Mitochondria and Cancer. Cell *166*, 555–566.
3. Weinberg, S.E., and Chandel, N.S. (2015). Targeting mitochondria metabolism for cancer therapy. Nat. Chem. Biol. *11*, 9–15.
4. Savic, L.J., Chapiro, J., Duwe, G., and Geschwind, J.F. (2016). Targeting glucose metabolism in cancer: new class of agents for loco-regional and systemic therapy of liver cancer and beyond? Hepat. Oncol. *3*, 19–28.
5. Lee, M., and Yoon, J.H. (2015). Metabolic interplay between glycolysis and mitochondrial oxidation: The reverse Warburg effect and its therapeutic implication. World J. Biol. Chem. *6*, 148–161.
6. Miyanishi, K., Tanaka, S., Sakamoto, H., and Kato, J. (2019). The role of iron in hepatic inflammation and hepatocellular carcinoma. Free Radic. Biol. Med. *133*, 200–205.
7. Yuan, X., Wang, B., Yang, L., and Zhang, Y. (2018). The role of ROS-induced autophagy in hepatocellular carcinoma. Clin. Res. Hepatol. Gastroenterol. *42*, 306–312.
8. Anastasiadou, E., Jacob, L.S., and Slack, F.J. (2018). Non-coding RNA networks in cancer. Nat. Rev. Cancer *18*, 5–18.
9. Zhao, Y., Sun, L., Wang, R.R., Hu, J.F., and Cui, J. (2018). The effects of mitochondria-associated long noncoding RNAs in cancer mitochondria: New players in an old arena. Crit. Rev. Oncol. Hematol. *131*, 76–82.
10. Dong, Y., Yoshitomi, T., Hu, J.F., and Cui, J. (2017). Long noncoding RNAs coordinate functions between mitochondria and the nucleus. Epigenetics Chromatin *10*, 41.
11. Rackham, O., Shearwood, A.M., Mercer, T.R., Davies, S.M., Mattick, J.S., and Filipovska, A. (2011). Long noncoding RNAs are generated from the mitochondrial genome and regulated by nuclear-encoded proteins. RNA *17*, 2085–2093.
12. Noh, J.H., Kim, K.M., Abdelmohsen, K., Yoon, J.H., Panda, A.C., Munk, R., Kim, J., Curtis, J., Moad, C.A., Wohler, C.M., et al. (2016). HuR and GRSF1 modulate the nuclear export and mitochondrial localization of the lncRNA RMRP. Genes Dev. *30*, 1224–1239.
13. Vendramin, R., Marine, J.C., and Leucci, E. (2017). Non-coding RNAs: the dark side of nuclear-mitochondrial communication. EMBO J. *36*, 1123–1133.
14. Zhao, Y., Liu, S., Zhou, L., Li, X., Meng, Y., Li, Y., Li, L., Jiao, B., Bai, L., Yu, Y., et al. (2019). Aberrant shuttling of long noncoding RNAs during the mitochondria-nuclear crosstalk in hepatocellular carcinoma cells. Am. J. Cancer Res. *9*, 999–1008.
15. Kim, J., Piao, H.L., Kim, B.J., Yao, F., Han, Z., Wang, Y., Xiao, Z., Siverly, A.N., Lawhon, S.E., Ton, B.N., et al. (2018). Long noncoding RNA MALAT1 suppresses breast cancer metastasis. Nat. Genet. *50*, 1705–1715.
16. Best, J., Schotten, C., Theysohn, J.M., Wetter, A., Müller, S., Radünz, S., Schulze, M., Canbay, A., Dechêne, A., and Gerken, G. (2017). Novel implications in the treatment of hepatocellular carcinoma. Ann. Gastroenterol. *30*, 23–32.
17. Kim, K.M., Noh, J.H., Abdelmohsen, K., and Gorospe, M. (2017). Mitochondrial noncoding RNA transport. BMB Rep. *50*, 164–174.
18. Buchan, K.D., Prajsnar, T.K., Ogryzko, N.V., de Jong, N.W.M., van Gent, M., Kolata, J., Foster, S.J., van Strijp, J.A.G., and Renshaw, S.A. (2019). A transgenic zebrafish line for in vivo visualisation of neutrophil myeloperoxidase. PLoS ONE *14*, e0215592.
19. Taxiarchis, A., Mahdessian, H., Silveira, A., Fisher, R.M., and Van't Hooft, F.M. (2019). PNPLA2 influences secretion of triglyceride-rich lipoproteins by human hepatoma cells. J. Lipid Res. *60*, 1069–1077.
20. Zhang, J., Han, C., Ungerleider, N., Chen, W., Song, K., Wang, Y., Kwon, H., Ma, W., and Wu, T. (2019). A Transforming Growth Factor-β and H19 Signaling Axis in Tumor-Initiating Hepatocytes That Regulates Hepatic Carcinogenesis. Hepatology *69*, 1549–1563.
21. Abbastabar, M., Sarfi, M., Golestani, A., and Khalili, E. (2018). lncRNA involvement in hepatocellular carcinoma metastasis and prognosis. EXCLI J. *17*, 900–913.
22. Li, X., Chen, N., Zhou, L., Wang, C., Wen, X., Jia, L., Cui, J., Hoffman, A.R., Hu, J.F., and Li, W. (2019). Genome-wide target interactome profiling reveals a novel *EEF1A1* epigenetic pathway for oncogenic lncRNA *MALAT1* in breast cancer. Am. J. Cancer Res. *9*, 714–729.
23. Chen, N., Zhao, G., Yan, X., Lv, Z., Yin, H., Zhang, S., Song, W., Li, X., Li, L., Du, Z., et al. (2018). A novel FLI1 exonic circular RNA promotes metastasis in breast cancer by coordinately regulating TET1 and DNMT1. Genome Biol. *19*, 218.
24. Jia, L., Wang, Y., Wang, C., Du, Z., Zhang, S., Wen, X., Zhou, L., Li, H., Chen, H., Li, D., et al. (2020). Oplr16 serves as a novel chromatin factor to control stem cell fate by modulating pluripotency-specific chromosomal looping and TET2-mediated DNA demethylation. Nucleic Acids Res. *48*, 3935–3948.
25. Murray, C.J., Ortblad, K.F., Guinovart, C., Lim, S.S., Wolock, T.M., Roberts, D.A., Dansereau, E.A., Graetz, N., Barber, R.M., Brown, J.C., et al. (2014). Global, regional, and national incidence and mortality for HIV, tuberculosis, and malaria during 1990-2013: a systematic analysis for the Global Burden of Disease Study 2013. Lancet *384*, 1005–1070.
26. Yu, D., Du, Z., Pian, L., Li, T., Wen, X., Li, W., Kim, S.J., Xiao, J., Cohen, P., Cui, J., et al. (2017). Mitochondrial DNA Hypomethylation Is a Biomarker Associated with Induced Senescence in Human Fetal Heart Mesenchymal Stem Cells. Stem Cells Int. *2017*, 1764549.
27. Clay Montier, L.L., Deng, J.J., and Bai, Y. (2009). Number matters: control of mammalian mitochondrial DNA copy number. J. Genet. Genomics *36*, 125–131.
28. Falkenberg, M. (2018). Mitochondrial DNA replication in mammalian cells: overview of the pathway. Essays Biochem. *62*, 287–296.

29. Milenkovic, D., Matic, S., Kühl, I., Ruzzenente, B., Freyer, C., Jemt, E., Park, C.B., Falkenberg, M., and Larsson, N.G. (2013). TWINKLE is an essential mitochondrial helicase required for synthesis of nascent D-loop strands and complete mtDNA replication. Hum. Mol. Genet. *22*, 1983–1993.

30. Ekstrand, M.I., Falkenberg, M., Rantanen, A., Park, C.B., Gaspari, M., Hultenby, K., Rustin, P., Gustafsson, C.M., and Larsson, N.G. (2004). Mitochondrial transcription factor A regulates mtDNA copy number in mammals. Hum. Mol. Genet. *13*, 935–944.

31. Sullivan, L.B., and Chandel, N.S. (2014). Mitochondrial reactive oxygen species and cancer. Cancer Metab. *2*, 17.

32. McArthur, K., Whitehead, L.W., Heddleston, J.M., Li, L., Padman, B.S., Oorschot, V., Geoghegan, N.D., Chappaz, S., Davidson, S., San Chin, H., et al. (2018). BAK/BAX macropores facilitate mitochondrial herniation and mtDNA efflux during apoptosis. Science *359*, eaao6047.

33. Xu, Z., Yang, L., Xu, S., Zhang, Z., and Cao, Y. (2015). The receptor proteins: pivotal roles in selective autophagy. Acta Biochim. Biophys. Sin. (Shanghai) *47*, 571–580.

34. Birgisdottir, A.B., Lamark, T., and Johansen, T. (2013). The LIR motif - crucial for selective autophagy. J. Cell Sci. *126*, 3237–3247.

35. Lazarou, M., Sliter, D.A., Kane, L.A., Sarraf, S.A., Wang, C., Burman, J.L., Sideris, D.P., Fogel, A.I., and Youle, R.J. (2015). The ubiquitin kinase PINK1 recruits autophagy receptors to induce mitophagy. Nature *524*, 309–314.

36. Heo, J.M., Ordureau, A., Paulo, J.A., Rinehart, J., and Harper, J.W. (2015). The PINK1-PARKIN Mitochondrial Ubiquitylation Pathway Drives a Program of OPTN/NDP52 Recruitment and TBK1 Activation to Promote Mitophagy. Mol. Cell *60*, 7–20.

37. Ahmad, S., Mu, X., Yang, F., Greenwald, E., Park, J.W., Jacob, E., Zhang, C.Z., and Hur, S. (2018). Breaching Self-Tolerance to Alu Duplex RNA Underlies MDA5-Mediated Inflammation. Cell *172*, 797–810.e13.

38. Marchese, D., de Groot, N.S., Lorenzo Gotor, N., Livi, C.M., and Tartaglia, G.G. (2016). Advances in the characterization of RNA-binding proteins. Wiley Interdiscip. Rev. RNA *7*, 793–810.

39. Buzaglo-Azriel, L., Kuperman, Y., Tsoory, M., Zaltsman, Y., Shachnai, L., Zaidman, S.L., Bassat, E., Michailovici, I., Sarver, A., Tzahor, E., et al. (2016). Loss of Muscle MTCH2 Increases Whole-Body Energy Utilization and Protects from Diet-Induced Obesity. Cell Rep. *14*, 1602–1610.

40. Maryanovich, M., Zaltsman, Y., Ruggiero, A., Goldman, A., Shachnai, L., Zaidman, S.L., Porat, Z., Golan, K., Lapidot, T., and Gross, A. (2015). An MTCH2 pathway repressing mitochondria metabolism regulates haematopoietic stem cell fate. Nat. Commun. *6*, 7901.

41. Zaltsman, Y., Shachnai, L., Yivgi-Ohana, N., Schwarz, M., Maryanovich, M., Houtkooper, R.H., Vaz, F.M., De Leonardis, F., Fiermonte, G., Palmieri, F., et al. (2010). MTCH2/MIMP is a major facilitator of tBID recruitment to mitochondria. Nat. Cell Biol. *12*, 553–562.

42. Amodio, N., Raimondi, L., Juli, G., Stamato, M.A., Caracciolo, D., Tagliaferri, P., and Tassone, P. (2018). MALAT1: a druggable long non-coding RNA for targeted anti-cancer approaches. J. Hematol. Oncol. *11*, 63.

43. Dennerlein, S., Wang, C., and Rehling, P. (2017). Plasticity of Mitochondrial Translation. Trends Cell Biol. *27*, 712–721.

44. McCormick, E.M., Muraresku, C.C., and Falk, M.J. (2018). Mitochondrial Genomics: A complex field now coming of age. Curr. Genet. Med. Rep. *6*, 52–61.

45. De Paepe, B., Lefever, S., and Mestdagh, P. (2018). How long noncoding RNAs enforce their will on mitochondrial activity: regulation of mitochondrial respiration, reactive oxygen species production, apoptosis, and metabolic reprogramming in cancer. Curr. Genet. *64*, 163–172.

46. Yoshimoto, R., Mayeda, A., Yoshida, M., and Nakagawa, S. (2016). MALAT1 long non-coding RNA in cancer. Biochim. Biophys. Acta *1859*, 192–199.

47. Toraih, E.A., Ellawindy, A., Fala, S.Y., Al Ageeli, E., Gouda, N.S., Fawzy, M.S., and Hosny, S. (2018). Oncogenic long noncoding RNA MALAT1 and HCV-related hepatocellular carcinoma. Biomed Pharmacother *102*, 653–669.

48. White, E., Mehnert, J.M., and Chan, C.S. (2015). Autophagy, Metabolism, and Cancer. Clin Cancer Res *21*, 5037–5046.

49. Vara-Perez, M., Felipe-Abrio, B., and Agostinis, P. (2019). Mitophagy in Cancer: A Tale of Adaptation. Cells *8*, 493.

50. Kulikov, A.V., Luchkina, E.A., Gogvadze, V., and Zhivotovsky, B. (2017). Mitophagy: Link to cancer development and therapy. Biochem. Biophys. Res. Commun. *482*, 432–439.

51. Dash, S., Sarashetti, P.M., Rajashekar, B., Chowdhury, R., and Mukherjee, S. (2018). TGF-β2-induced EMT is dampened by inhibition of autophagy and TNF-α treatment. Oncotarget *9*, 6433–6449.

52. Staff, P.G.; PLOS Genetics Staff (2016). Correction: fMiRNA-192 and miRNA-204 Directly Suppress lncRNA HOTTIP and Interrupt GLS1-Mediated Glutaminolysis in Hepatocellular Carcinoma. PLoS Genet. *12*, e1005825.

53. Redis, R.S., Vela, L.E., Lu, W., Ferreira de Oliveira, J., Ivan, C., Rodriguez-Aguayo, C., Adamoski, D., Pasculli, B., Taguchi, A., Chen, Y., et al. (2016). Allele-Specific Reprogramming of Cancer Metabolism by the Long Non-coding RNA CCAT2. Mol. Cell *61*, 640.

54. Li, H.J., Li, X., Pang, H., Pan, J.J., Xie, X.J., and Chen, W. (2015). Long non-coding RNA UCA1 promotes glutamine metabolism by targeting miR-16 in human bladder cancer. Jpn. J. Clin. Oncol. *45*, 1055–1063.

55. Yang, F., Zhang, H., Mei, Y., and Wu, M. (2014). Reciprocal regulation of HIF-1α and lincRNA-p21 modulates the Warburg effect. Mol. Cell *53*, 88–100.

56. Li, X., Zhao, Q., Qi, J., Wang, W., Zhang, D., Li, Z., and Qin, C. (2018). lncRNA Ftx promotes aerobic glycolysis and tumor progression through the PPARγ pathway in hepatocellular carcinoma. Int. J. Oncol. *53*, 551–566.

57. Kong, L., Zhou, X., Wu, Y., Wang, Y., Chen, L., Li, P., Liu, S., Sun, S., Ren, Y., Mei, M., et al. (2015). Targeting HOTAIR Induces Mitochondria Related Apoptosis and Inhibits Tumor Growth in Head and Neck Squamous Cell Carcinoma in vitro and in vivo. Curr. Mol. Med. *15*, 952–960.

58. Goding, C.R. (2016). Targeting the lncRNA SAMMSON Reveals Metabolic Vulnerability in Melanoma. Cancer Cell *29*, 619–621.

59. Leucci, E., Vendramin, R., Spinazzi, M., Laurette, P., Fiers, M., Wouters, J., Radaelli, E., Eyckerman, S., Leonelli, C., Vanderheyden, K., et al. (2016). Melanoma addiction to the long non-coding RNA SAMMSON. Nature *531*, 518–522.

60. Luo, F., Liu, X., Ling, M., Lu, L., Shi, L., Lu, X., Li, J., Zhang, A., and Liu, Q. (2016). The lncRNA MALAT1, acting through HIF-1α stabilization, enhances arsenite-induced glycolysis in human hepatic L-02 cells. Biochim. Biophys. Acta *1862*, 1685–1695.

61. Wilusz, J.E., Freier, S.M., and Spector, D.L. (2008). 3′ end processing of a long nuclear-retained noncoding RNA yields a tRNA-like cytoplasmic RNA. Cell *135*, 919–932.

62. Barrey, E., Saint-Auret, G., Bonnamy, B., Damas, D., Boyer, O., and Gidrol, X. (2011). Pre-microRNA and mature microRNA in human mitochondria. PLoS ONE *6*, e20220.

63. Geiger, J., and Dalgaard, L.T. (2018). Isolation and Analysis of Mitochondrial Small RNAs from Rat Liver Tissue and HepG2 Cells. Methods Mol. Biol. *1782*, 337–350.

64. Sun, J., Li, W., Sun, Y., Yu, D., Wen, X., Wang, H., Cui, J., Wang, G., Hoffman, A.R., and Hu, J.-F. (2014). A novel antisense long noncoding RNA within the IGF1R gene locus is imprinted in hematopoietic malignancies. Nucleic Acids Res. *42*, 9588–9601.

65. Kim, S.J., Mehta, H.H., Wan, J., Kuehnemann, C., Chen, J., Hu, J.F., Hoffman, A.R., and Cohen, P. (2018). Mitochondrial peptides modulate mitochondrial function during cellular senescence. Aging (Albany NY) *10*, 1239–1256.

66. Shults, C.L., Dingwall, C.B., Kim, C.K., Pinceti, E., Rao, Y.S., and Pak, T.R. (2018). 17β-estradiol regulates the RNA-binding protein Nova1, which then regulates the alternative splicing of estrogen receptor β in the aging female rat brain. Neurobiol. Aging *61*, 13–22.

OMTN, Volume *23*

Supplemental Information

Nuclear-Encoded lncRNA *MALAT1* Epigenetically Controls Metabolic Reprogramming in HCC Cells through the Mitophagy Pathway

Yijing Zhao, Lei Zhou, Hui Li, Tingge Sun, Xue Wen, Xueli Li, Ying Meng, Yan Li, Mengmeng Liu, Shanshan Liu, Su-Jeong Kim, Jialin Xiao, Lingyu Li, Songling Zhang, Wei Li, Pinchas Cohen, Andrew R. Hoffman, Ji-Fan Hu, and Jiuwei Cui

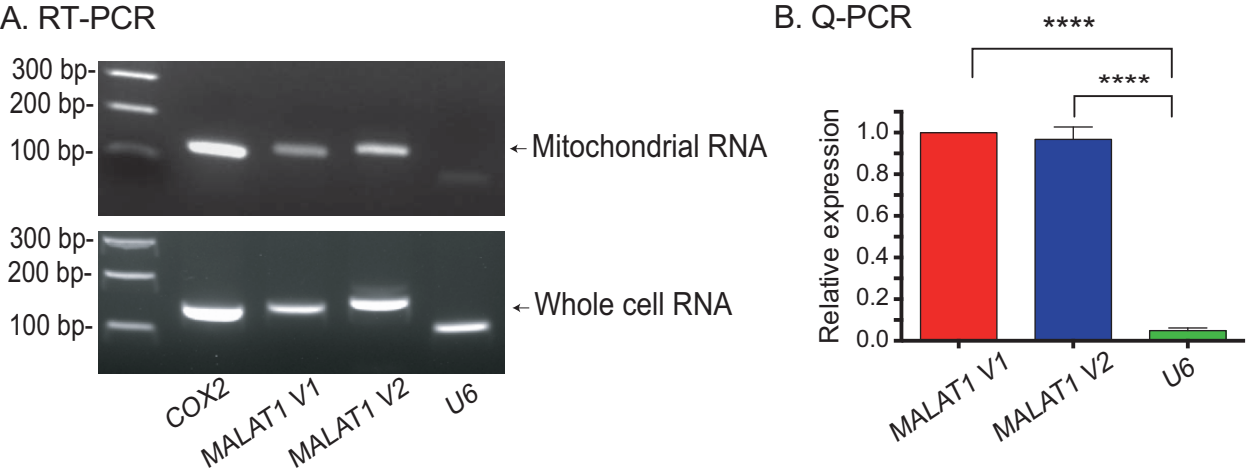

Figure S1. Quality check of isolated mitochondria.

A.Quality check of isolated mitochondria RNA. RT-PCR was used to examine the quality of isolated mitochondrial RNAs for the contamination of nuclear U6 RNA. V1, V2: PCR primers for two MALAT1 variants. The whole cell RNAs were used as the control. MALAT1 and mitochondrial control COX2 were abundantly detected in isolated HepG2 mitochondria RNA. No nuclear U6 was detected in mitochondrial RNA samples. B.Q-PCR quantitation of MALAT1 in isolated mitochondria RNA. The nuclear MALAT1 were highly enriched in HepG2 mitochondria.

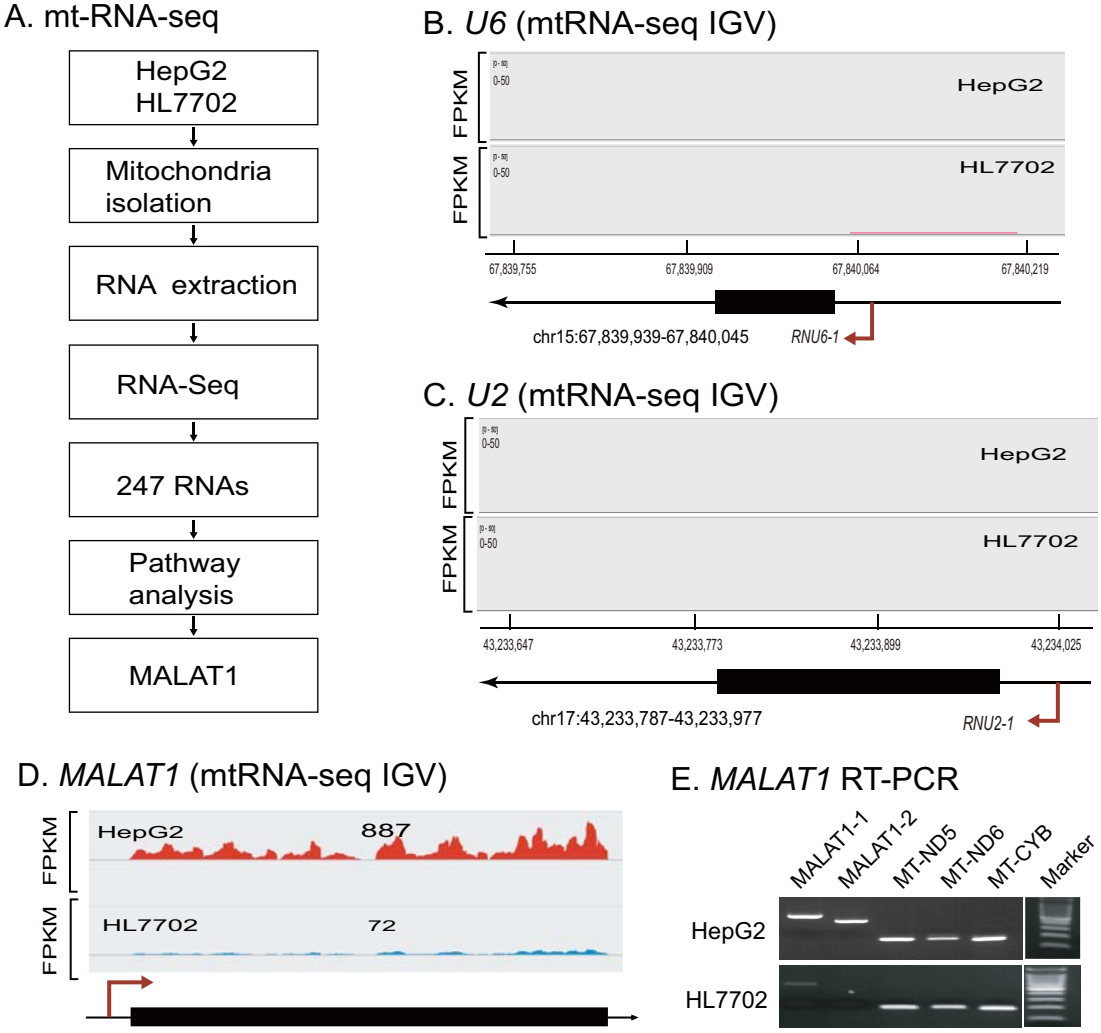

Figure S2. MALAT1 is enriched in the mitochondria of hepatoma cells.
A. Flow chart of RNA-sequencing to identify RNAs in isolated mitochondria; B. Quality check of RNA-seq data for nuclear U6 RNA. IGV Sashimi blot shows the absence of U6 RNA in the HepG2 mitochondria RNA-seq dataset; C. Quality check of RNA-seq data for nuclear U2 RNA. U2 RNA is absent in HepG2 mitochondria RNA-seq data; D. IGV Sashimi blot of MALAT1. MALAT1 is highly enriched in hepatoma HepG2 mitochondria compared with normal hepatic HL7702 mitochondria; E. RT-PCR analyses of MALAT1 and mitochondrial gene transcripts in isolated mitochondrial RNAs. MALAT1-1, MALAT1-2: RT-PCR for two different MALAT1 variants. MT-ND5, MT-ND6, MT-CYB: mitochondrial gene transcripts as the PCR controls.

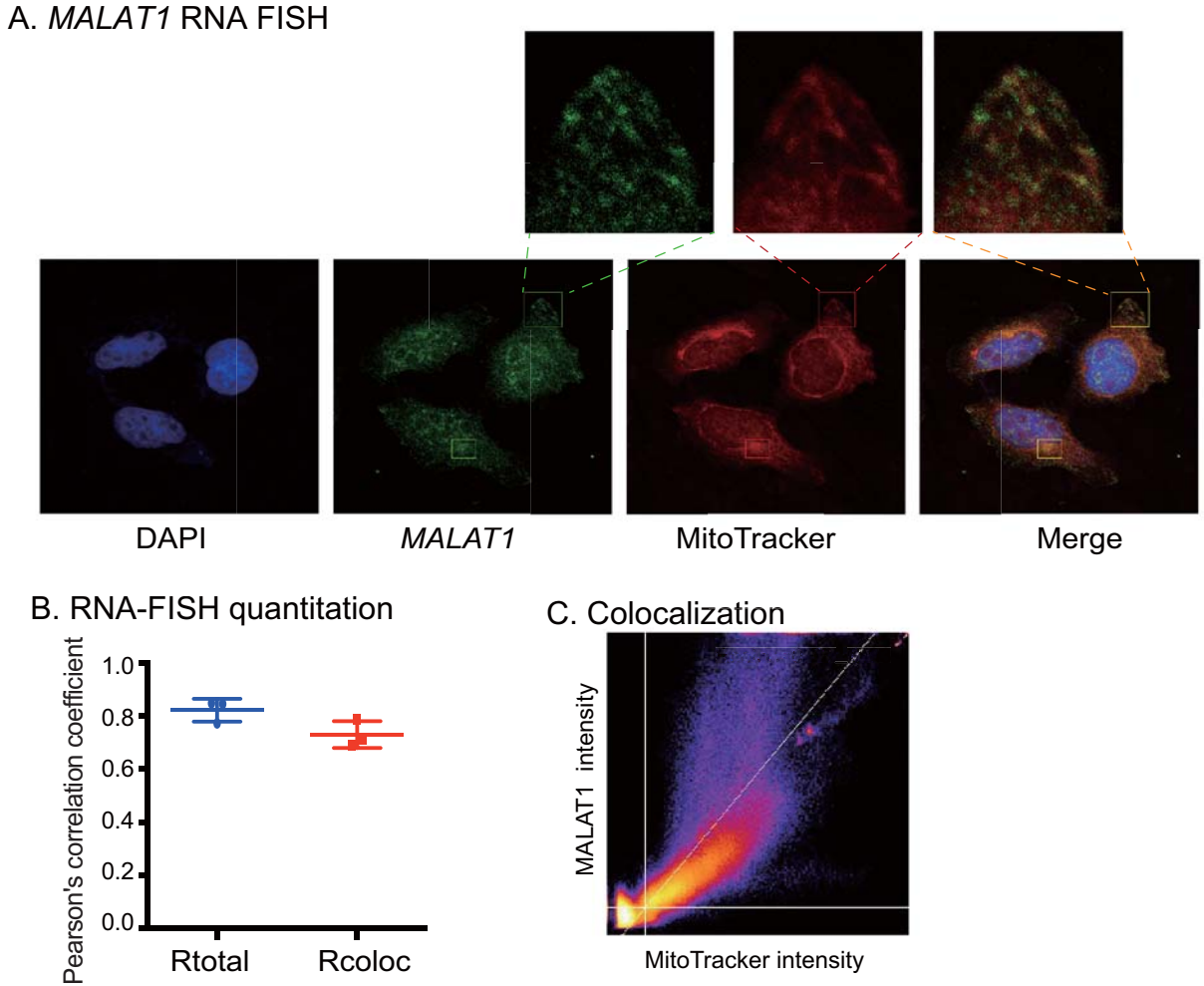

Figure S3. MALAT1 RNA FISH using antisense single stranded DNA probes.
A. RNA-FISH of mitochondria-associated MALAT1 in HepG2 cells. Dig-labeled single stranded MALAT1 probes were synthesized by asymmetric PCR and were used for hybridization with FITC-coupled anti-dig antibody (green). Mitochondria were labeled with MitoTracker (red).B. Quantitation of MALAT1 and MitoTracker. Pearson's correlation coefficient was measured for the entire image (Rtotal) and the pixels above thresholds (Rcoloc) from 3 tested field of views. C. Scatter plot of channel 1 (MALAT1, green) and channel 2 (MitoTracker, red). The regression line is plotted along with the threshold level for channel 1 (vertical line) and channel 2 (horizontal line). Mean +/- SEM are indicated in the right upper corner of the image.

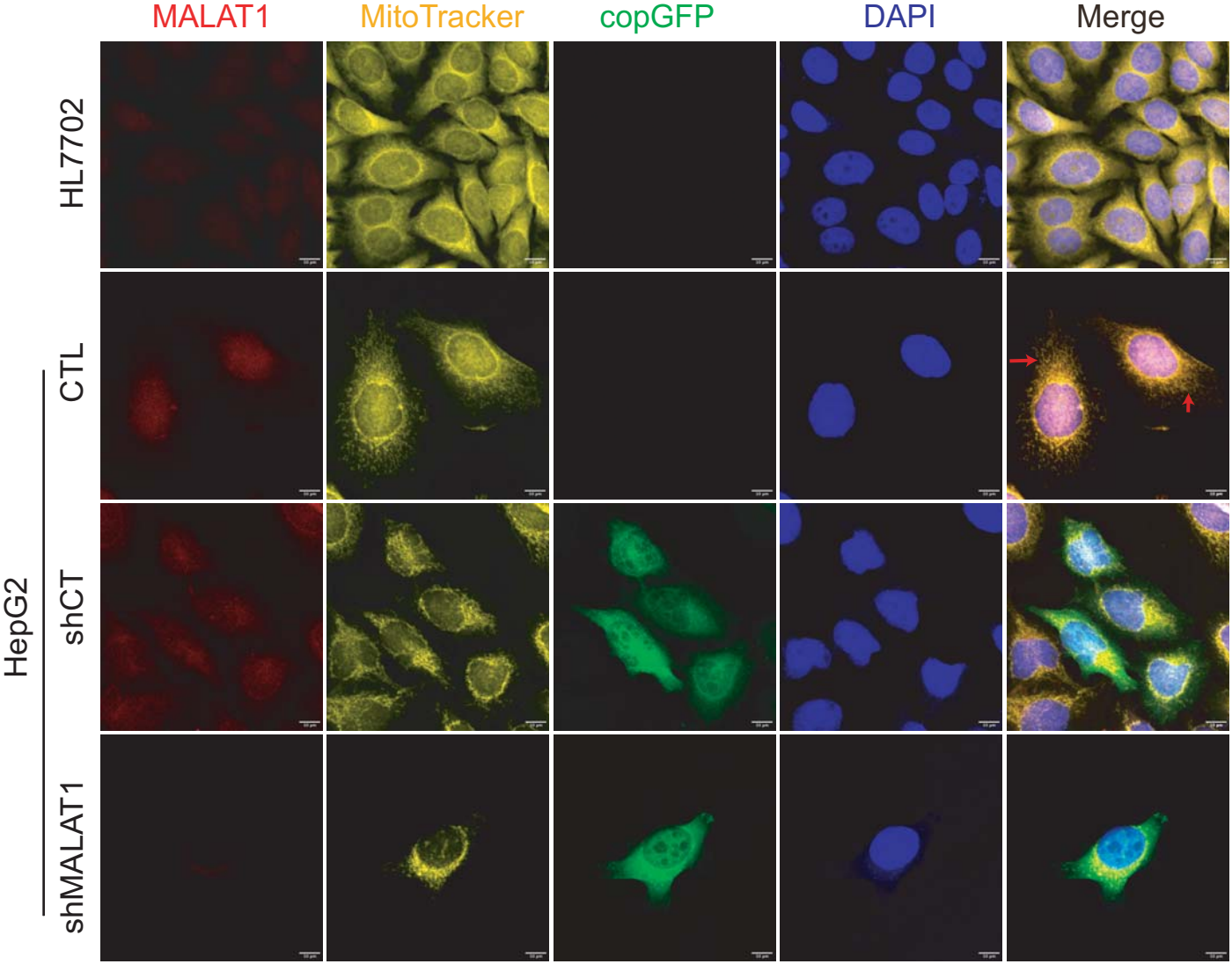

Fig.S4 RNA-FISH of MALAT1 in HL7702 and shRNA-treated HepG2 cells.
MALAT1 was probed with antisense oligonucleotide probes (red) provided in the Ribo Fluorescent In Situ Hybridization Kit (C10910, RiboBio). Mitochondria were labeled with MitoTracker (yellow). Cells were counterstained with DAPI and imaged under a confocal laser-scanning microscope (Carl Zeiss). HL7702: normal hepatic cells; shMALAT1, shCT: HepG2 cells transfected with lentiviruses carrying shMALAT1, shRNA control (shCT); CTL: untreated HepG2 cells; copGFP: the track marker in the lentiviral vector (green). Red arrow: Co-localization of lncRNA MALAT1 and MitoTracker.

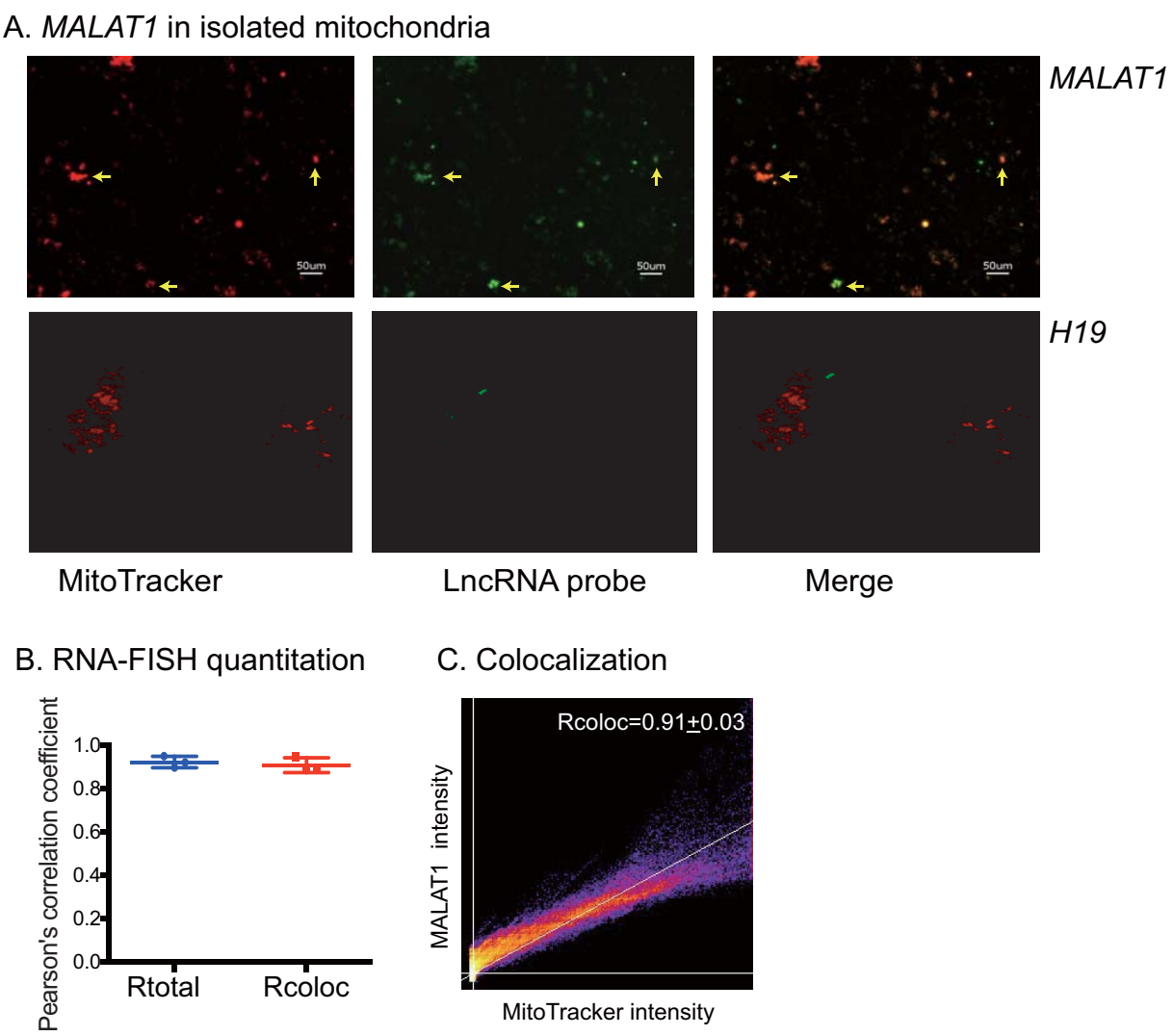

Figure S5. *MALAT1* **and** *H19* **RNA FISH in isolated mitochondria.**
A. Co-localization of MALAT1 and MitoTracker in isolated mitochondria smear. Mitochondria were isolated and smeared on slides for RNA FISH detection of MALAT1 (green). Mitochondria were tracked by MitoTracker staining (red). B. Quantitation of MALAT1 and MitoTracker in isolated mitochondria smear. Pearson's correlation coefficient was calculated for the entire image (Rtotal) and the pixels above thresholds (Rcoloc) from 3 tested field of views. C. Scatter plot of channel 1 (MALAT1, green) vs. channel 2 (MitoTracker, red). The regression line is plotted along with the threshold level for channel 1 (vertical line) and channel 2 (horizontal line). Mean +/- SEM are indicated in the right upper corner of the image.

A. *MALAT1* knockdown

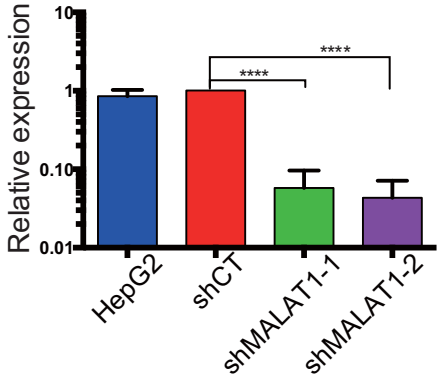

B. MT-DNA CpG island

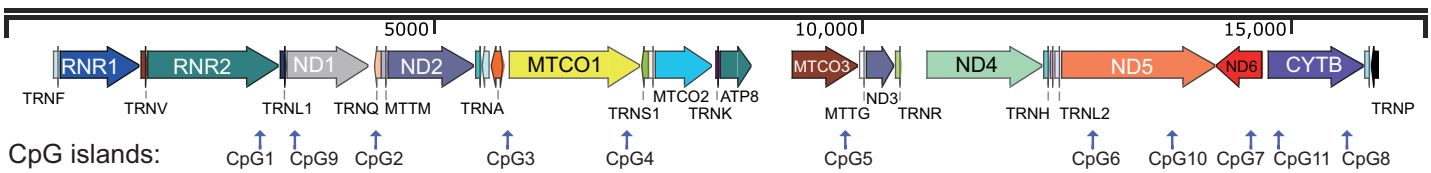

C. MT-DNA methylation

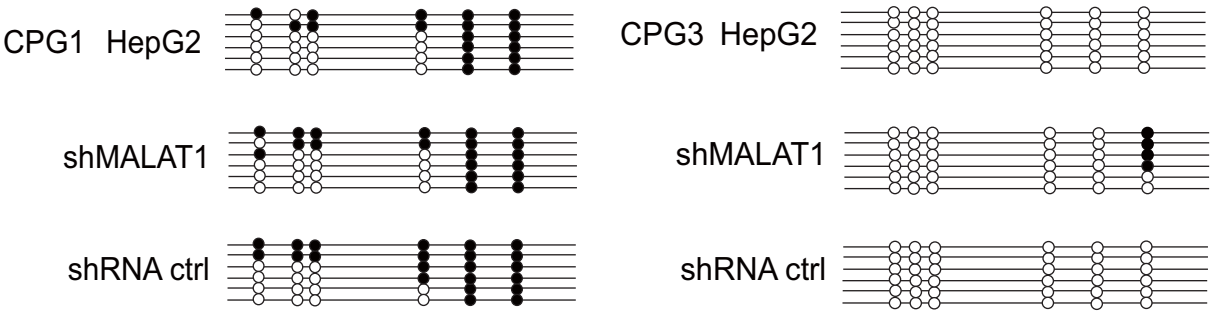

Figure S6. ***MALAT1*** **knockdown and mitochodnrial DNA methylation**

A. MALAT1 knockdown by shRNAs in HepG2 cells. shMALAT1-1, shMALAT1-2: MALAT1 shRNAs; shCT: random shRNA control. MALAT1 was quantitated by Q-PCR. The Ct value was normalized over that of β-ACTIN (housekeeping gene) and then standardized by setting shCT as 1 for comparison. **** P<0.0001 compared with the shCT group, one-way ANOVA, followed by student t test.

B. Location of CpG islands in the mitochondrial DNA genome. C. The status of CpG methylation. Sodium bisulfite pre-treated mitochondria DNA used EZ DNA methylation kit to detect the MALAT1 binding region methylation. Black dots, methylated CpG sites; white dots, unmethylated CpG sites.

A.Mitochondria number under TEM

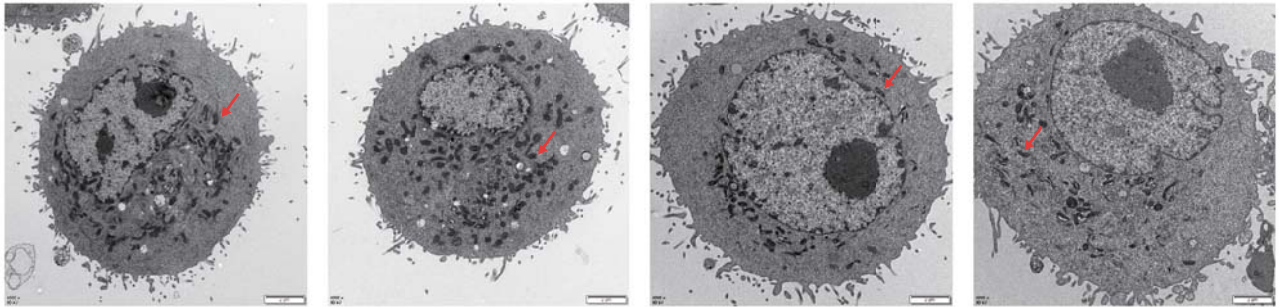

Figure S7. MALAT1 knockdown rduced mitochondria DNA copy number in HepG2 cells. Mitochondria quantity and modality were observed under Transmission electronic microscope (TEM). Red arrow: mitochondria under TEM. Mitochondria per cell was quantitated in Figure 2E.

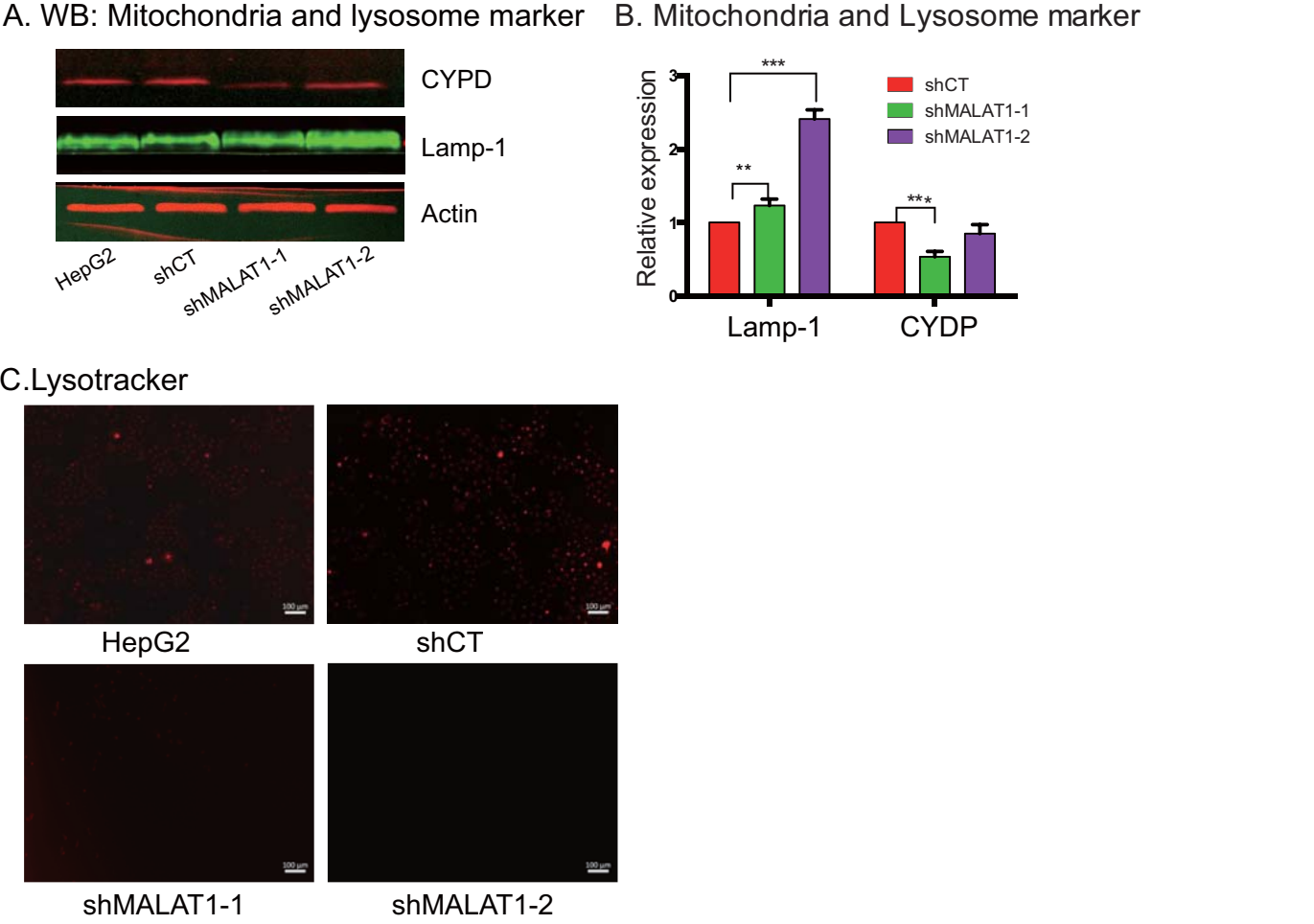

Figure S8. MALAT1 knockdown impaired the mitophagy pathway.
A. Mitochondria and lysosome by Western blot. The quantity of mitochondria was assessed by mitochondria membrane marker CYPD and lysosome by lysosome marker Lamp-1. MALAT1 knockdown cells (shMALAT1-1 and shMALAT1-2) show decreased mitochondria membrane marker CYPD and increased lysosome marker Lamp-1; B. Quantitation of CYPD and Lamp-1 Western blot results. ** P<0.01, *** P<0.001compared with controls; C.Acidic lysosome staining by Lysotracker. Reduced acidic lysosomes were observed in shMALAT1-treated HepG2 cells.

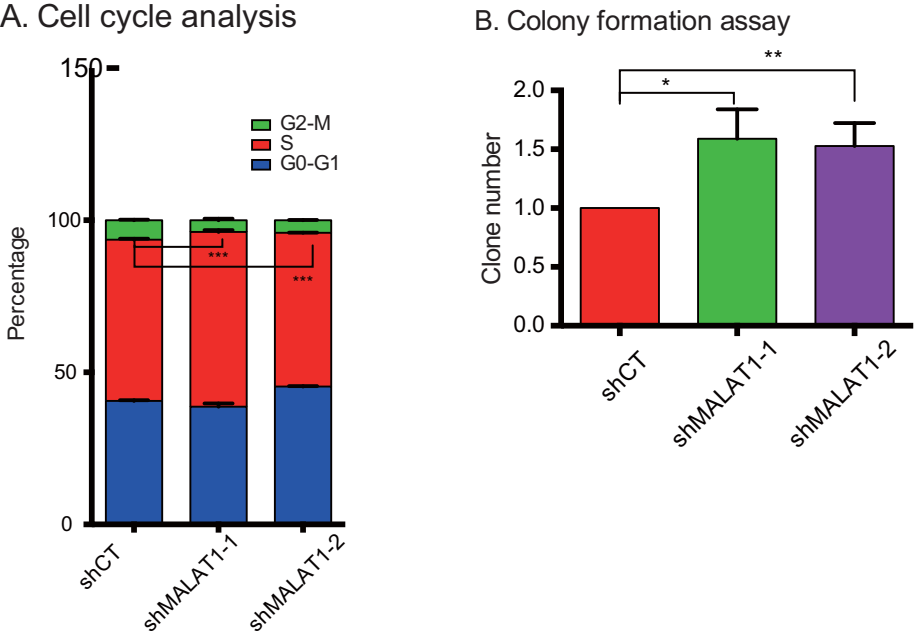

Figure S9. MALAT1 knockdown affect cell cycle and colony formation.
A. Cell cycle analysis. MALAT1 knockdown cells (shMALAT1-1 and shMALAT1-2) showed less on G2 stage compared to shCT. *** P<0.001 compared with the control group. B. Clone formation assay. MALAT1 knockdown cells (shMALAT1-1 and shMALAT1-2) showed more clone formation ability compared to the shCT group. * P=0.0149, ** P<0.01 compared with t he control group.

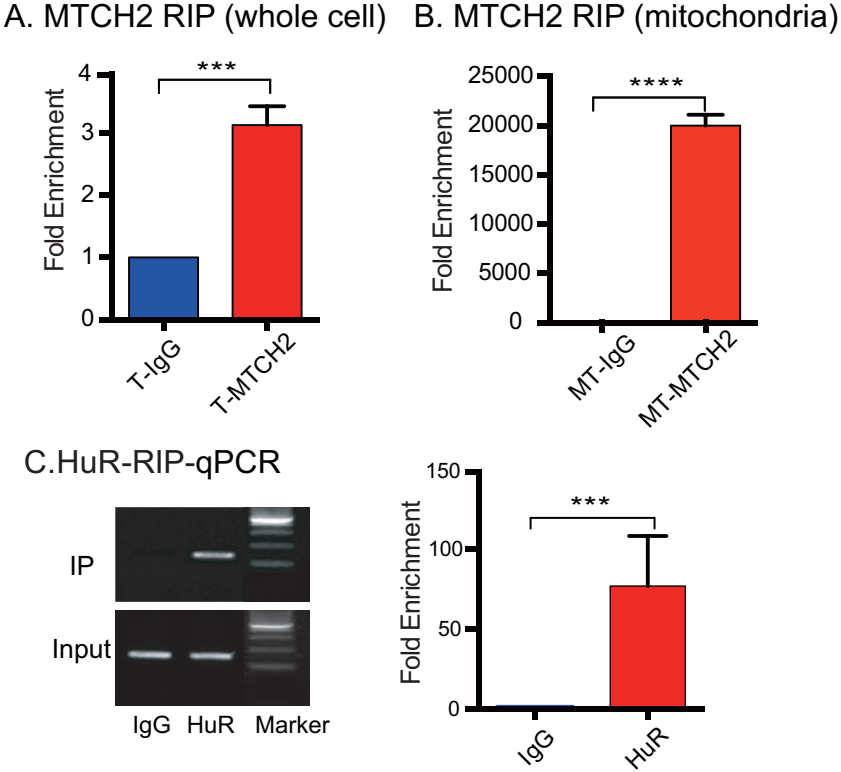

Figure S10. Putative transportation of MALAT1 in mitochondria.

A. Interaction of MALAT1 with mitochondria membrane protein MTCH2 in the whole cell lysate. The interaction was assessed by RIP. *** $P<0.001$ compared with the IgG control group. B. MALAT1 interaction with MTCH2 in mitochondria lysate. **** $P<0.0001$ compared with the IgG control group. C. Interaction of MALAT1 with RNA transporter protein HuR. The interaction was detected by RIP PCR and Q-PCR. *** $P<0.001$ compared with the IgG control group.

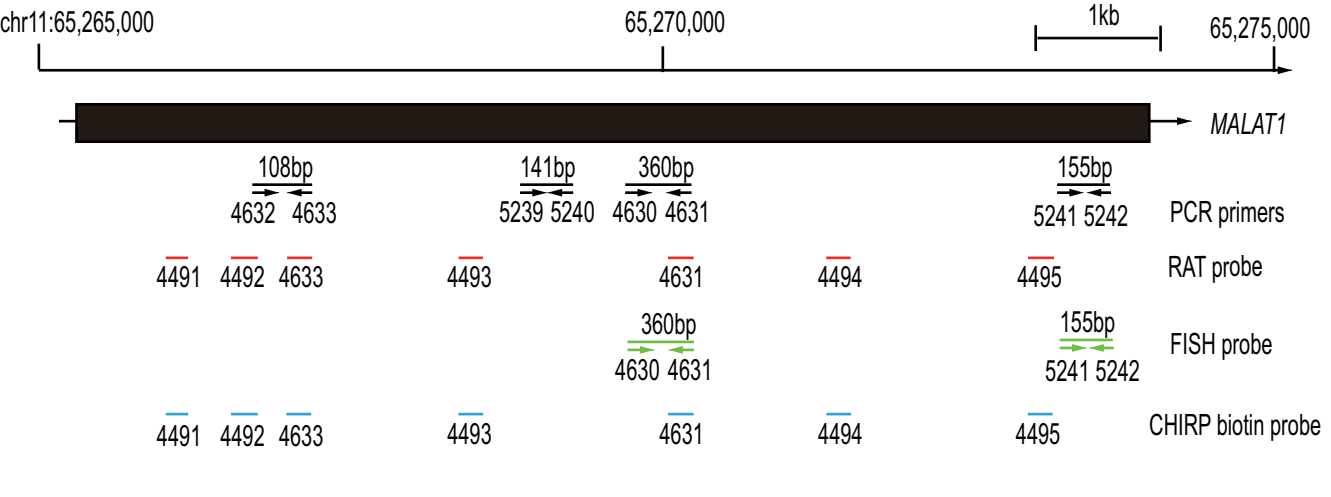

Figure S11. Location of RAT, CHIRP, FISH probes and PCR primers in the MALAT1 locus. The daigraam shows the chr11:65,265,000-65,275,000 region, where the MALAT1 gene is located. The scale bar is 1kb. Arrows: the direction of PCR primer or probe oligonucletides. Red arrow: RAT probes; blue arrow: CHIRP probes; green arrow: FISH probe; black arrow: PCR primers. RAT and CHIRP probes are labled with biotin.